SANDIA REPORT
SAND2006-24952495
Unlimited Release
Printed April 2006

A Science-Based Understanding of Cermet Processing

John. N. Stuecker, Joseph. Cesarano III, Kimberly. A. Shollenberger, R. Allen Roach, Alice C. Kilgo, Donald F. Susan, David. J. Van Ornum

Prepared by
Sandia National Laboratories
Albuquerque, New Mexico 87185 and Livermore, California 94550

Sandia is a multiprogram laboratory operated by Sandia Corporation,
a Lockheed Martin Company, for the United States Department of Energy's
National Nuclear Security Administration under Contract DE-AC04-94AL85000.

Issued by Sandia National Laboratories, operated for the United States Department of Energy by Sandia Corporation.

Available to DOE and DOE contractors from
U.S. Department of Energy
Office of Scientific and Technical Information
P.O. Box 62
Oak Ridge, TN 37831

Telephone: (865) 576-8401
Facsimile: (865) 576-5728
E-Mail: reports@adonis.osti.gov
Online ordering: http://www.osti.gov/bridge

Available to the public from
U.S. Department of Commerce
National Technical Information Service
5285 Port Royal Rd.
Springfield, VA 22161

Telephone: (800) 553-6847
Facsimile: (703) 605-6900
E-Mail: orders@ntis.fedworld.gov
Online order: http://www.ntis.gov/help/ordermethods.asp?loc=7-4-0#online

SAND2006-24952495X
Unlimited Release
Printed April 2006X

A Science-Based Understanding of Cermet Processing

J. N. Stuecker, J. Cesarano III
Ceramic Materials Center

K. A. Shollenberger, R. A. Roach
Engineering Sciences Center

A.C. Kilgo, D. F. Susan
Materials Characterization

D. J. Van Ornum
Development Builds

Sandia National Laboratories
P.O. Box 5800
Albuquerque, NM 87185-01349

Abstract

This report is a summary of the work completed in FY01 for science-based characterization of the processes used to fabricate 1) cermet vias in source feedthrus using slurry and paste-filling techniques and 2) cermet powder for dry pressing. Common defects found in cermet vias were characterized based on the ability of subsequent processing techniques (isopressing and firing) to remove the defects. Non-aqueous spray drying and mist granulation techniques were explored as alternative methods of creating CND50, the powder commonly used for dry pressed parts. Compaction and flow characteristics of these techniques were analyzed and compared to standard dry-ball-milled CND50. Due to processing changes, changes in microstructure can occur. A microstructure characterization technique was developed to numerically describe cermet microstructure. Machining and electrical properties of dry pressed parts were also analyzed and related to microstructure using this analytical technique.

Executive Summary

This report outlines accomplishments in the science-based understanding of cermet processing up to fiscal year 2002 for Sandia National Laboratories. The three main areas of work are centered on 1) increasing production yields of slurry-filled cermets, 2) evaluating the viability of high-solids-loading pastes for the same cermet components, and 3) optimizing cermet powder used in pressing processes (CND50). An additional development that was created as a result of the effort to fully understand the impacts of alternative processing techniques is the use of analytical methods to relate microstructure to physical properties. Recommendations are suggested at the end of this report. Summaries of these four efforts are as follows:

1. Increase Production Yields of Slurry-Filled Cermet Vias

   Finalized slurry filling criteria were determined based on three designs of experiments where the following factors were analyzed: vacuum time, solids loading, pressure drop across the filter paper, slurry injection rate, via prewetting, slurry injection angle, filter paper prewetting, and slurry mixing time. Many of these factors did not have an influence on defect formation. In order of decreasing importance, critical factors for defect formation by slurry filling are vacuum time (20 sec. optimal), slurry solids loading (20.0 g of cermet with 13.00 g of DGBEA solvent (21.2 vol%)), filling with the pipette in a vertical position, and faster injection rates (~765 μl/s) as preferable to slower.

   No further recommendations for improvement to this process can be suggested. All findings of the slurry filling process have been transferred to CeramTec, the supplier. Paste filling methods appear to show more promise of increasing production yields.

   The types of flaws commonly found in slurry-filled vias were identified and followed throughout the entire source feedthru process. In general, all sizes of cracks healed during isopressing and firing steps. Additionally, small to medium sized voids (less than 1/3 the via diameter) can be healed. Porosity will usually lead to via necking, which may cause the part to be out of specification. Large voids (greater

than 1/3 of the diameter) and partial fills are not healed or produce significant necking.

2. Viability of High-Solids-Loading-Cermet Paste for Filling Source Feedthru Via

   The paste-filling process is easy to implement and easier to use. The high solids loading (>40 vol %) reduces the incidence of drying defects, which are seen in slurry filled (~23 vol %) vias. Additionally, the way in which the vias are filled (the paste is pushed from entrance to exit, displacing air as the paste front progresses), reduces the chance of entrapped voids, which are common in the slurry filling process. From the fair number of samples already filled, the likelihood of this process being a viable and reliable process is very good. Issues of concern for the paste process, as with any new process, are any problems that may arise in subsequent manufacturing stages of the neutron tube that may be affected by subtle changes in microstructure. Both MC4277 and MC4300-type source feedthrus were paste-filled by hand. X-ray analysis showed a much lower existence of voids in the green parts as compared to slurry-filled parts. The paste shows improvements in shelf life (weeks) as compared to slurry (minutes).

   This method of introducing the cermet to the via also lends itself very well to an automated filling process where a machine can either drill vias or, with the aid of a vision system, find pre-drilled vias and fill them with paste. The pastes used in this work prove the concept of this automated filling process as MC4277 sources have been filled using such a prototype machine, however, better performing pastes can be developed which are less hazardous (aqueous systems). The paste process was also used to successfully fill MC4300 “dogleg” type sources.

3. Optimize CND50

   Two methods of creating granulated cermet powder for comparison with dry-ball milled CND50 were explored. The first method, non-aqueous spray drying, was performed at Niro Inc. used a 40/60 (wt %) ethanol/toluene solvent and three binder systems; polyvinyl butyral (B79), ethylcellulose (Ethocel), and hydroxypropylcellulose (Klucel). Due to the nature of small spray-dry systems, an excess amount of fines was present in the granulated powder, which may have contributed to the low angles of repose (68 to 78°). This is a moderate increase in

flowability as standard dry-ball milled powder possesses an angle of repose of 79-89°. Mist granulated powders were produced with a tert-butanol solvent and polyvinyl butyral binder system. The angles of repose were more promising (28°). More investigation into the mist granulation method is required. Also, aqueous spray drying may be possible with cermet and should be explored. Compaction of all granulated powders is much closer to a proven pressing powder (Sandi94 – angle of repose 29°) which should allow cermet to be pressed to near net shape where die filling is difficult for non-flowing powders.

4. Microstructure Characterization

An analytical technique was developed to numerically characterize microstructures in terms of molybdenum dispersion, homogeneity, and percolation indices. This technique was applied to dry-ball-milled samples of various ball-milling times (0.5 to 20 hours). Significant change in the microstructure could be seen with milling time. Increased milling time caused agglomeration of molybdenum particles, increasing the percolation index, whereas short milling times promoted higher dispersion indices. This phenomenon is contrary to conventional understanding of mixing. However, conventional ball milling does not usually incorporate granules with binder and separate particles. This discrepancy may explain the odd mixing behavior.

It is important to note that the high percolation index possessed by long ball mill times showed lower electrical resistance than low-percolation-index microstructures. However, machinability of high percolation, low-dispersion-index microstructures were poor as compared to microstructures with high dispersion indices and moderate percolation indices. This trade-off between dispersion and percolation (at constant molybdenum levels) suggests that microstructures can be achieved that posses good mechanical and electrical properties. Coincidentally, microstructures that satisfy this condition are produced by the standard dry-ball-milled CND50 (4 hour ball mill time).

The performance and sensitivity of the microstructure characterization technique should be evaluated, specifically for electrical conductivity. Processing techniques to decrease the percolation index (lowering molybdenum content, excess ball milling,

larger molybdenum particles, etc.) should be employed to determine the point where cermet is not conductive or falls below electrical conduction specifications.

Table Of Contents

List of Figures

List of Tables

1. Introduction

Alumina/molybdenum CND50 cermet is used extensively in the production of neutron generator components. From source and target feedthrus comprised of co-fired cermet and alumina ceramic to solid flanged rings, the 50/50 wt% alumina/molybdenum cermet is critical in providing electrically conductive hermetic seals. There are two processing pathways cermet powder may follow during neutron generator part production. Both paths start with 4-8 μm molybdenum particles and 50-100 μm Sandi94 spray-dried granules which are blended together in a dry-ball-milling (DBM) process. The first path incorporates a solvent (diethylene glycol monobutyl ether acetate – DGBEA) and cermet powder to form a slurry or paste, which is then used to vacuum-fill a feedthru via. A previously generated SAND report goes into a detailed background of source feedthru filling, specifically for the MC4277 source.[1] The second, and more often used path, takes the cermet powder immediately to a dry-pressing or isopressing step in which slugs of cermet are created and then machined in the unsintered state to yield parts that can then be sintered and ground to in-specification neutron generator parts. The primary concern with this dry processing method is the compaction behavior of Mo powder (not optimal for dry-pressing) 'blended' with Sandi94 alumina granules (optimal for dry-pressing if by itself). The relevant work instruction (WI-704191-030 found in Appendix A) for dry blending leaves room for interpretation concerning how to blend the Mo and Sandi94 powders. As a result, very different CND50 may result from this blending process, which will then affect all cermet parts.

A few critical variables concerning slurry-filling source feedthrus were incorporated into a first design of experiments in the previous SAND report[1] with the goal of bracketing processing parameters for slurry filling operators (WI-704191-040 found in Appendix B) . However, from that study came several new variables of concern. Experiments using those variables in a second and third design of experiments are described in this report. Further, initial steps in creating a high-solids-loading-cermet paste for the intended use in defect-free via filling are reported.

Within Sandia, CND50 preparation has been optimized for the particular processing setup being used. This setup requires following procedures such as monitoring the speed of the ball mill used to blend the powders and defining the powder

batch size. Both procedures are not followed in the industrial setting of CeramTec (Laurens, SC, USA) where larger batches are created. Batch sizes at CeramTec are 2.742 kg. It has been seen qualitatively that the blending procedure will have a great influence on machinability of dry-pressed parts. Thus, compaction behavior and microstructure of the Sandia processed CND50, termed 'standard' CND50, must be characterized to insure a similar product is created, regardless of processing procedure. Blending procedures are analyzed in this report with analytical tool developed specifically for this problem. This tool allows microstructures to be quantitatively characterized by mathematical algorithms and optical analytical techniques.

2. Work Objectives

Increase Production Yields of Slurry-Filled Cermet Vias

In order to increase production yields, several processing parameters identified by previous findings[1] were investigated. Such processing parameters are the possibility of pre-wetting the vias, changing the orientation of the slurry-dispensing tip, and altering the amount of time the slurry-filled via is exposed to vacuum just after the via has been filled. From this study, other processing parameters were identified and include pre-wetting the filter paper located between the via and vacuum source and correlating the via fill integrity with the age of the slurry. All insights from this study were transferred to CeramTec to aid in increasing production yields.

During the analysis of slurry filled vias, it was noted that some flaws created during vacuum filling would 'heal' during the subsequent isopressing procedure. This discovery led to the characterization of all voids, some which would heal and others that would not.

Viability of High-Solids-Loading-Cermet Paste for Filling Source Feedthru Vias

The current method of via filling, which incorporates a vacuum assist, inherently entraps voids within the filled via. Further, it is unclear if the cermet, starting as a 23.5% dense material, fully densifies during additional processing steps (isopressing and sintering). The ideal situation for via filling is to somehow fill the empty via with a void free material, which then compacts in a similar manner with the surrounding alumina

during the isopressing step. In order to meet these goals, higher solids loading slurries, termed pastes for distinction, must be utilized. The method for introducing these pastes into the via in a controlled manner must be determined.

Optimize CND 50

Dry-ball-milling (DBM) time has a significant effect on the resulting machinability of the unfired cermet and electrical conductivity of the sintered cermet. A design of experiments was created to determine critical factors in green machining, grinding, and electrical conductivity. In addition to DBM, non-aqueous spray-drying and mist granulation were used to create homogeneous granules of CND50 instead of simply blending the Mo powder and alumina granules together. The idea behind creating homogeneous granules is to ensure mixing of the Mo and alumina phases while producing a flowable CND50 powder (as the standard DBM CND50 does not fill molds well). The non-aqueous spray drying was performed in collaboration with CeramTec. Mist granulation was performed at Sandia.

Once any new cermet blends are created, their compaction behavior should be at least as good as the standard CND50 blend to ensure that there are no negative changes in dry-pressed-cermet part creation. For example, mold filling should be as good if not better, and parts should exhibit similar, if not higher density, than the standard CND50 blend after compaction. As compaction is not the only criteria by which the CND50 should be evaluated, a quantitative analytical method was employed to characterize resulting microstructures of each new blend. Parameters such as homogeneity, dispersion, and phase percolation were compared and contrasted among the blends. Further, these parameters were related to measurable physical characteristics such as green machinability and conductivity.

3. General Materials and Materials Preparation

Via Filling Experiments

Cermet slurry is created in accordance to the work instruction WI-704191-040, with 4 hour DBM CND50 and DGBEA as the solvent (SS305003-200). No other organics or dispersants were added to the slurry. Alumina compacts 0.875 in. diameter

were used (SS305195) with vias drilled to specification. An automatic pipette (Rainin, Oakland, Ca, USA) was used to deposit slurry into the via in a controlled manner.

Cermet pastes were created using the standard Mo powder and Sandi94 that had been calcined to 600°C/4 hrs to remove all organics, bringing the alumina back from granule form to primary particles. The powders were combined with a soluble binder, Butvar B79 (Solutia, St. Louis, Mo, USA), and blended in a mechanical mixer (paint shaker) until smooth (0.5-1 hours). The cermet paste was injected into vias using a standard 10 mL syringe and a small piece of fitted silicone tubing that served as a sealing gasket between the syringe and alumina compact.

Flaws within the cermet via that were created during slurry filling were identified using pictures from microfocus X-ray at Sandia.

CND50 Preparation

The standard experimental setup at Sandia for dry-ball-milling CND50 uses a 250 ml polyethylene jar with 250g of 0.5" alumina milling media and 250g of Mo/Sandi94 rotating on a ball mill at 71 RPM for 4 hours. A slightly different setup is used at CeramTec to create larger batches. The CND50 blend is then sieved to separate it from the milling media. Dry-ball-milled CND50 was evaluated after isopressing in ~2' long rubber tubes, ~1.5 inches in diameter, with aluminum end caps. Machining of isopressed CND50 used diamond tooling to increase tool life.

Non-aqueous spray drying was performed at Niro Inc. (Columbia, MD, USA) on a 1.5 kg spray dryer. Several materials systems were attempted, all of which used denatured ethanol mixed with toluene as a solvent. Binders investigated were Butvar B79, Klucel E, Carbowax, and Ethocel. Dibutyl pthalate was used as a plasticizer. Dispersants used were Solsperse 24000 (Avecia, Wilmington, DE, USA), and PEI (Polysciences, Warrington, PA, USA).

Mist granulation was performed using a Thermal Technologies ultrasonic horn. The slurry was pumped to the ultrasonically vibrating tip by means of a peristaltic pump through silicone tubing. The solvent used was tert-butanol with a freezing point of 26°C and P_{vap} of 31 mm Hg. A magnetic stirrer was used to keep the slurry homogeneous in a beaker until it was drawn into the peristaltic pump. Slurry droplets were collected in a

liquid nitrogen bath and freeze dried in a vacuum chamber connected to a solvent trap and an oil vacuum pump.

Microstructures of fired CND50 were obtained from optical microscopy and characterized using IMAGIST (Princeton Gamma-Tech, Princeton, NJ) image analysis software.

4. Via Flaw Identification and Evaluation

Several types of flaws can be found in a filled via before isopressing. Some of these flaws are removed completely during the isopressing procedure with only a few clues to their presence remaining. These non-critical flaws do not affect the final part dimensions. Other flaws, termed critical flaws, however, cannot be completely removed with isopressing without causing the via to fall out of specification. Flaws can be voids formed during the filling process, cracks created during drying and consolidation, finely distributed porosity, or partial fills. Flaws of each type in green parts were revealed by microfocus X-ray. These parts were then isopressed and again X-rayed to determine the effects of each flaw type and size on the final via. Actual real-time video of the slurry filling process into an alumina compact has been performed and reveals the formation origins of these flaws.[2]

Table 1 outlines the types of flaws seen in slurry-filled vias. Critical flaws are highlighted in italics. Small cracks are defined as cracks less than half the height of the via section (either large diameter or small diameter section) they are in. Medium cracks are defined as cracks greater than half the section's length. Large cracks extend the entire section length. Small voids are typically less than 1/4 of the section's diameter. Medium voids approach 1/3 of the diameter, large voids are ~1/2 the diameter, while partial fills are ~3/4 of the diameter or greater. Porosity is defined as regions of low density not attributed to the presence of voids. One specific void position, in the transition area corner, is examined due to the high frequency of these voids in production parts.

Figure 1 through Figure 4 show the evolution of identified flaws from the green state to the isopressed state. From this analysis, it is easy to see that the small via is less likely to be healed regardless of the starting flaw. The reason for this is evident in Figure 2c and d. Isopressing moves the dry, consolidated cermet toward the center of the part,

with the large diameter via having more room for particle movement; the medium void can be filled in by the cermet, reducing the height of the via. This can only be seen here because the domes of cermet that are normally present above the via were removed for this particular study. If the domes were present, they would act as a material reservoir for filling the vias without compromising the overall size of the via. However, Figure 2d shows the large-diameter via on the left slightly shorter than the large-diameter via on the right caused by filling in the medium void. Therefore, fairly large-sized voids can be healed in the large-diameter via, but even small voids cannot be healed in the small-diameter via due to lower mobility of particles.

Although certain flaws may be healed during isopressing, the best way to obtain a high density via is to begin with no voids in the via.

Table 1: Flaw Nomenclature and Effect on Via

Defect Location	Defect Type	Results After Isopressing
Large Via	Large Crack	Healed
	Medium Crack	Healed
	Small Crack	Healed
	Large Void	***Moderate Necking at Point of Void***
	Medium Void	Healed
	Small Void	Healed
	Corner Void	Healed
	Porosity	***Moderate Necking***
	Partial Fill	***Very Large Void but may be Connected***
Small Via	***Large Crack***	***Moderate Necking at Point of Void***
	Medium Crack	Healed
	Small Crack	Healed
	Large Void	***Loss of Visible Connectivity***
	Medium Void	***Major Necking at Point of Void***
	Small Void	***Moderate Necking at Point of Void***
	Pipe Fill	***Major Necking***
	Porosity	***Major to Moderate Necking***
	Partial Fill	***Loss of Visible Connectivity***

* Flaws in bold are critical flaws that are not healed during isopressing

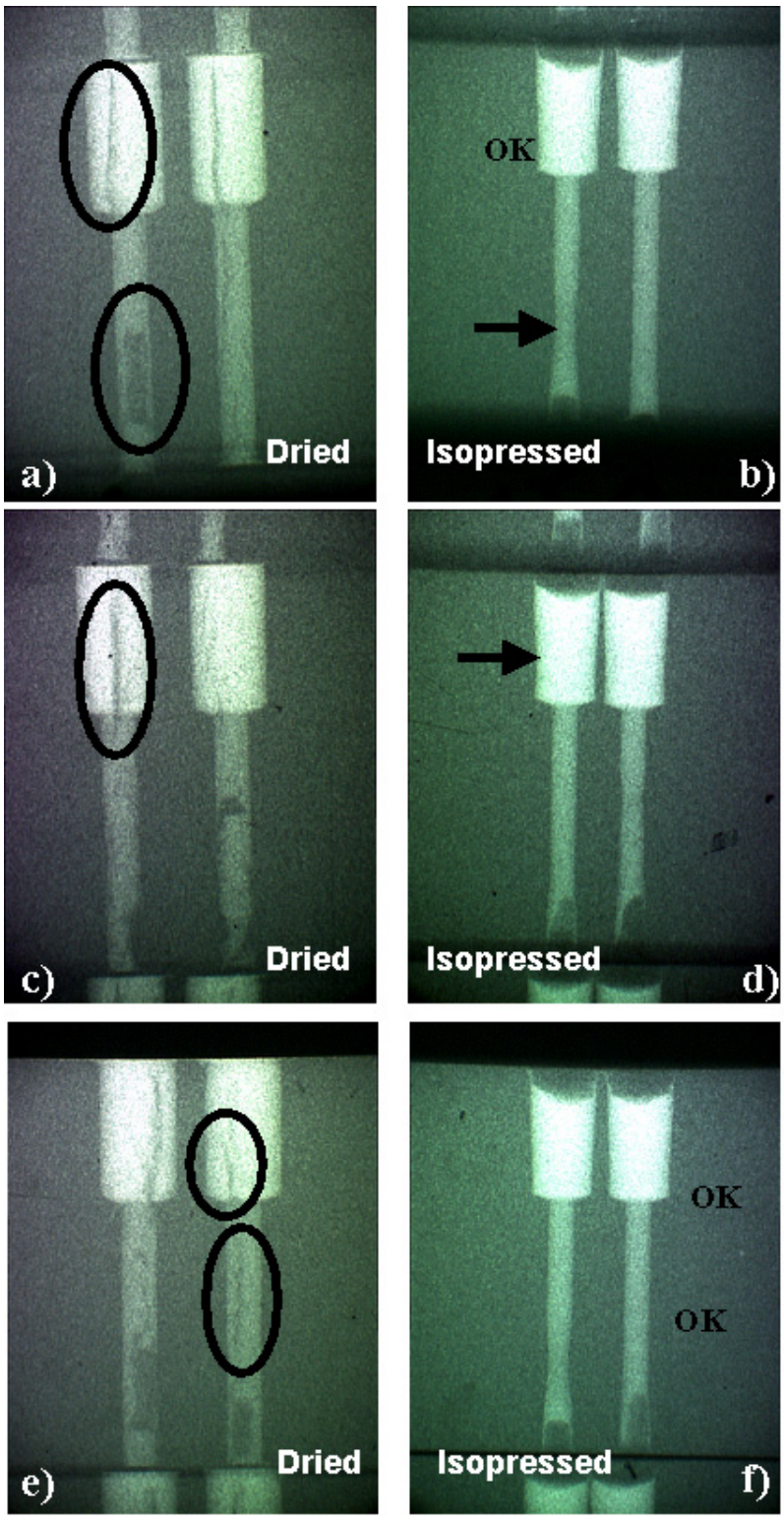

Figure 1: a) Large crack in large diameter via, medium void in small diameter via, c) medium crack in the large diameter via, e) small crack in large diameter via and medium crack in small diameter via before and after isopressing.

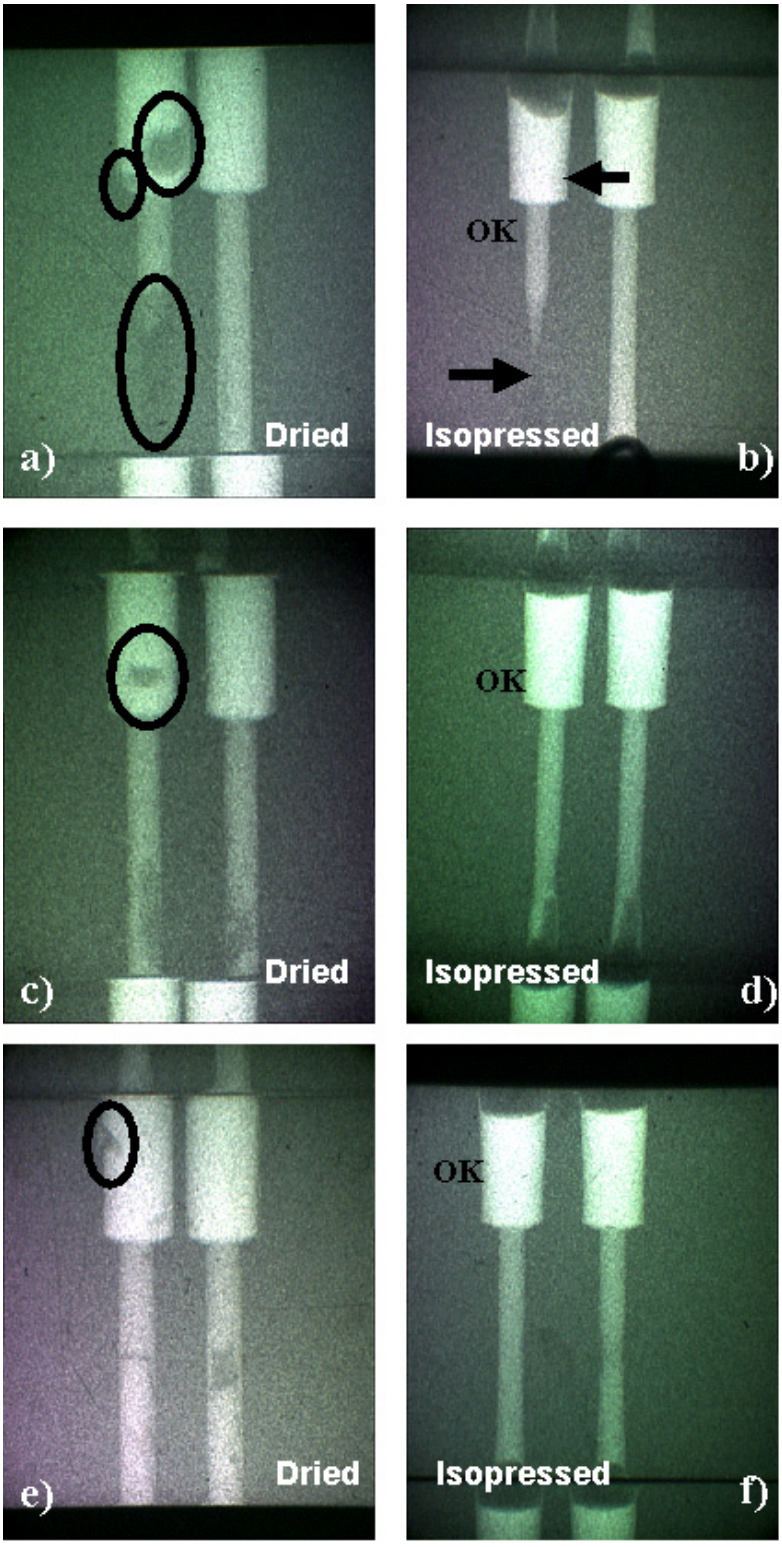

Figure 2: a) Large void in large diameter via, a corner void, and a partial fill in the small diameter via, c) medium void in the large diameter via, e) small void in the large diameter via before and after isopressing.

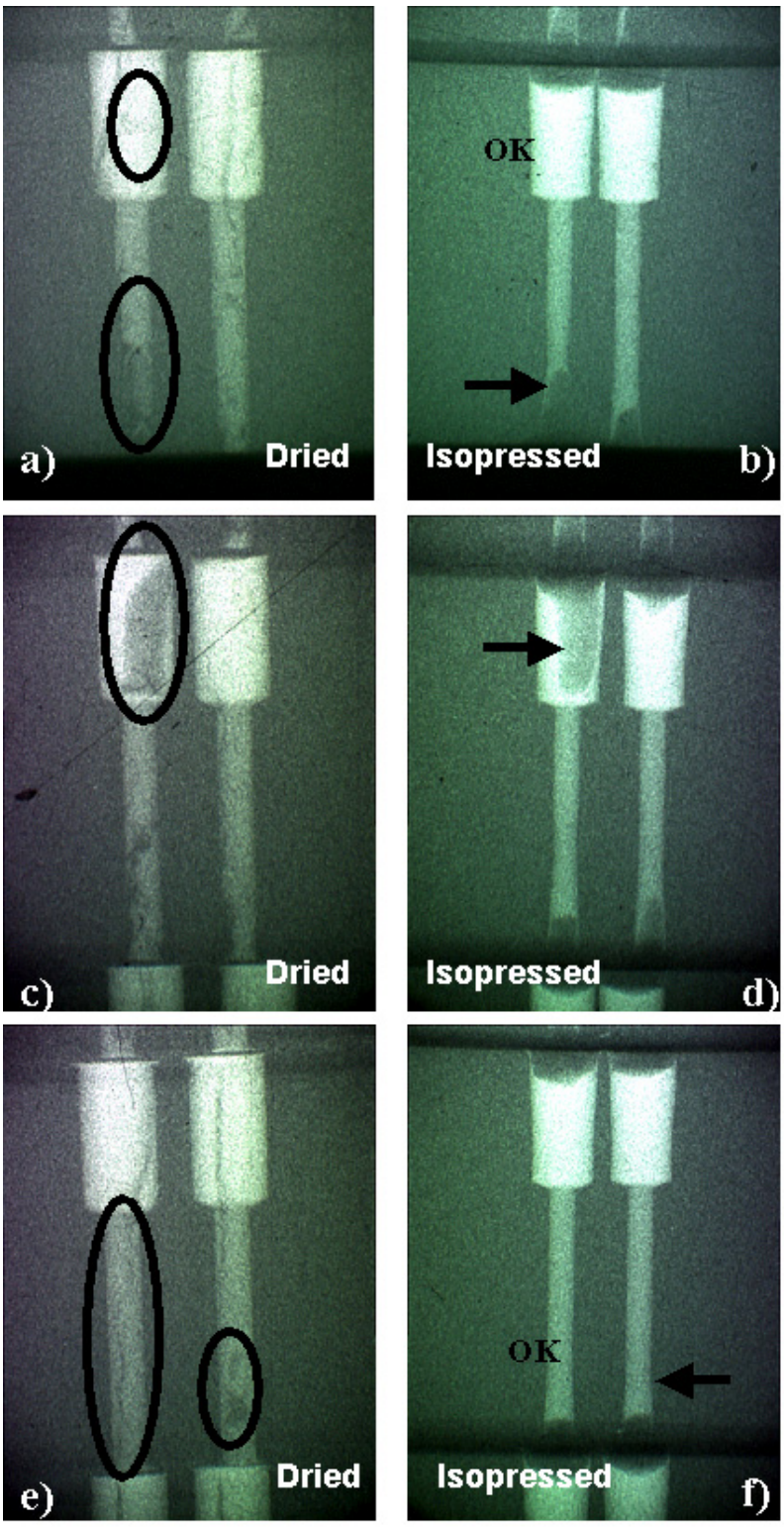

Figure 3: a) Porosity in the large diameter via and a large void in the small via, c) partial fill in the large diameter via, e) a large crack and small void in the small diameter via before and after isopressing.

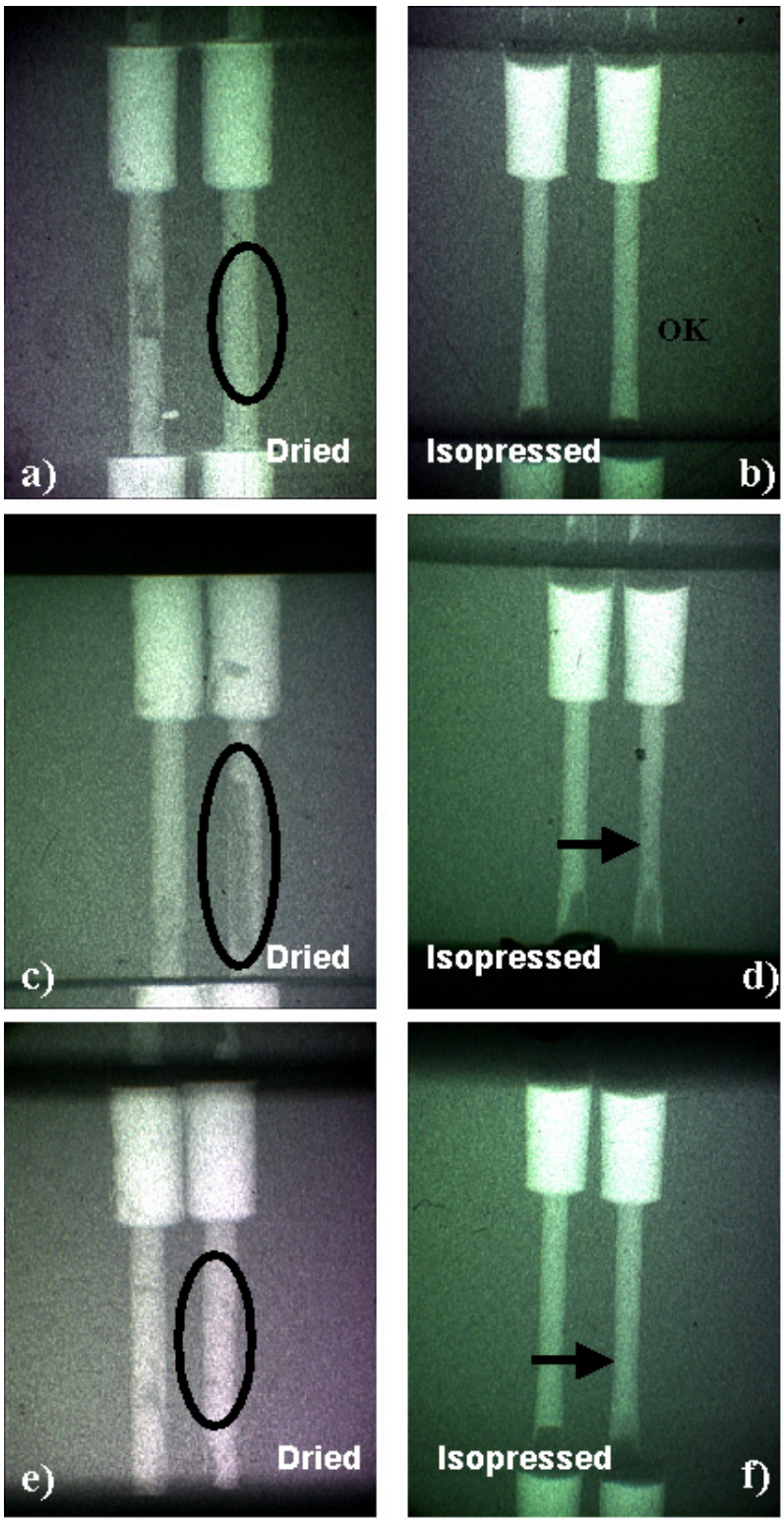

Figure 4: a) A small crack in the small diameter via, c) pipe fill in the small diameter via, e) porosity in the small diameter via before and after isopressing.

5. Increase Production Yields of Slurry-Filled Cermet Vias

Second Design Of Experiments

Factor Selection – DOE II

The first design of experiments (DOE I) performed in previous work[1] examined the effects of slurry concentration, vacuum pressure, vacuum time, and slurry injection rate into the via. The most influential factor in achieving a defect-free via is allowing the part to experience vacuum for at least 20 sec. Therefore, the second design of experiments (DOE II) incorporated increasing the vacuum time to 60 sec. It is believed that a longer vacuum time will allow further healing of the voids entrapped in the still flowable slurry before imbibition dries out and hardens the slurry.

Experienced operators have settled on holding the syringe tip at approximately a 45° angle to the alumina compact. Operators have found that by carefully rolling the slurry over the edge of the via under vacuum, more uniform fills can be created. DOE I used a fixture to insure a 45° angle with the compact. This same fixture was modified to hold the automatic pipette vertically in DOE II. It is hypothesized that a seal can be formed by the well-centered slurry drop to the top of the via. Then, the entire drop can be pulled into the via as one, in contrast to the turbulent effect seen visually during manual filling.

The third factor used in DOE II also came about from results of previous work.[1] It was determined that solvent imbibition from the via into the pressed compact would be complete in approximately 60 sec with no applied vacuum.[3] This time is much shorter if vacuum is constantly applied to the via (vacuum-driven imbibition). Therefore holding the via at vacuum for 60 seconds should not heal voids as the slurry would be dry and non-flowable well before the 60 seconds have elapsed. Therefore the third factor is via pre-wetting. If the area surrounding the slurry is already saturated with solvent, there will be less driving force for imbibition out of the slurry. Additionally, if the vacuum is pulling solvent out of the via and into, for instance, the filter paper, there will be a reservoir of solvent available within the compact to feed the slurry in the via, possibly allowing more time for the vacuum to remove voids from a flowable slurry. Holes were pre-wet with 1000 μl of solvent just prior to filling.

Experimental Design Matrix – DOE II

A statistical design of experiments was created using vacuum time (20 and 60 sec), filling angle (45° or vertical), and pre-wetting (pre-wet or not pre-wet) to create a 2^3 factorial (eight experiments) set of experiments, using 5 repetitions per experiment and two vias per repetition. Those eight experiments yielded 80 vias for analysis. The defect-presence analysis was conducted using maximum-likelihood estimation to estimate values of model parameters and their significance of producing a defect. Modules in Statistical Analysis Software, Proc Catmod and Proc Logistic, were used for analysis on defect formation.[1]

Experimental Procedure - DOE II

The slurry was created in accordance with the work instruction (WI-704191-050 Appendix B). 20.0 g of CND50 was combined with 11.56 g of DGBEA and mixed in a rotating cup at ~60 RPM for 30 minutes. The mixing cup contained nine stainless steel ball bearings to aid in mixing. One to two drops of DGBEA were added to the slurry after 30 minutes, until clicking of the mixing balls were heard. The vias were filled one at a time with the offset via being filled first. If pre-wetting was required, only the via to be filled was pre-wet. A foot pedal operated solenoid was used to release vacuum to the part after the prescribed amount of time had elapsed. The pipette fixture was changed according to the prescribed angle of the tip to the part (45° or vertical).

Statistical Results – DOE II

The response variable was set to the presence or absence of defects in both the large and small diameter sections of the via. The influence of each factor (pipette orientation, vacuum time, pre-wetting) is reported as a probability value (p-value). Small p-values imply higher significance of influence on the response variable. Table 2 shows the results on defect presence in the large diameter section of the via for each factor. From extensive previous results, it was determined that the large diameter section of the via yields representative data for the experiment.[1]

Table 2: DOE II Statistical Results

Via Location	Variable	Large Diameter	Small Diameter
Off-Center Via	Pre-wetting	NE	NE
	Vertical	NE	NE
	Vacuum Time	NE	NE
Center Via	Prewetting	NE	NE
	Vertical	NE	0.02*
	Vacuum Time	0.02+	NE

NE = No Effect
* vertical fill is better
+ 20 sec vacuum time is better

From Table 2, the two factors that had a positive influence on reducing defect formation were vertical filling and holding vacuum for 20 sec, not 60 sec. All other factors had neither a positive nor negative effect on defect formation.

Third Design of Experiments

Factor Selection – DOE III

The final design of experiments investigated a few factors that change during actual filling of many (up to ~100) source feedthrus. In the production setting, cermet slurry is kept in the rotating mixing cup with stainless steel media for several hours, often not in use. For example, a proficient operator can fill 100 source feedthrus in about two hours, however, scheduled work breaks, lunch breaks, or unforeseen delays may push the mixing time for the slurry up to four hours. This increase in mixing time has a thickening effect on the slurry. Operators have noticed the visual change in slurry rheology with time and have compensated by adding a few drops of solvent to the mixture.

Figure 5 shows the effect of mixing time on viscosity. It is not believed that the solvent is evaporating because the increase in viscosity can be seen when the mixing pot is tightly capped; further, the very low vapor pressure of DGBEA (P_{vap} = 0.01 mmHg at 20°C) reduces the likelihood of evaporation. Therefore it is thought that the powder morphology is changing with mixing time. Although the binder that holds the Sandi94

alumina spray-dried granules together is not soluble in DGBEA, the mechanical mixing provided by the steel milling media causes breakdown of the granules (Figure 6), altering the overall flow properties of the slurry. Therefore, mixing time was set as a factor. These mixing times were performed on the standard 23.3 vol% slurries as well as 21.2 vol% slurries.

During the first two designs-of-experiments, it was noticed that after the first via was filled, the Whatman 541 filter paper located between the via and vacuum source was spot-wet with DGBEA. This wetting could potentially have an adverse effect on filling the second via if vacuum through the saturated section of the filter paper is reduced. Therefore, a third factor, pre-wetting the filter paper, was added to finalize DOE III.

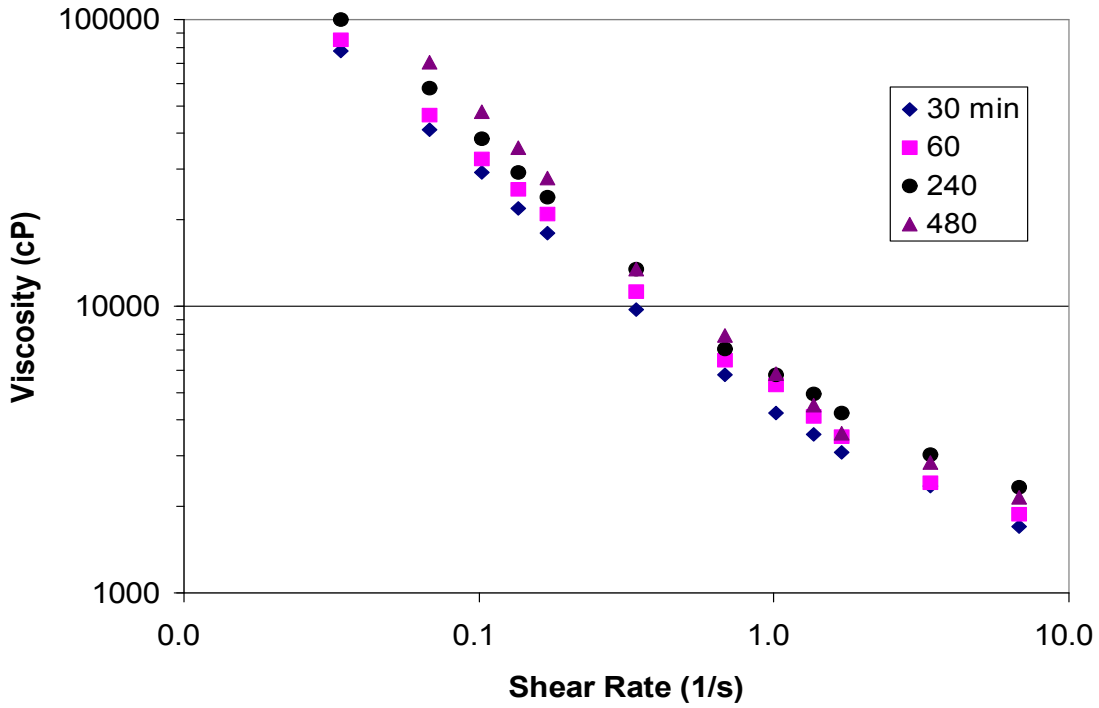

Figure 5: Viscosity vs. mixing time for a 23.5 vol% solids cermet slurry.

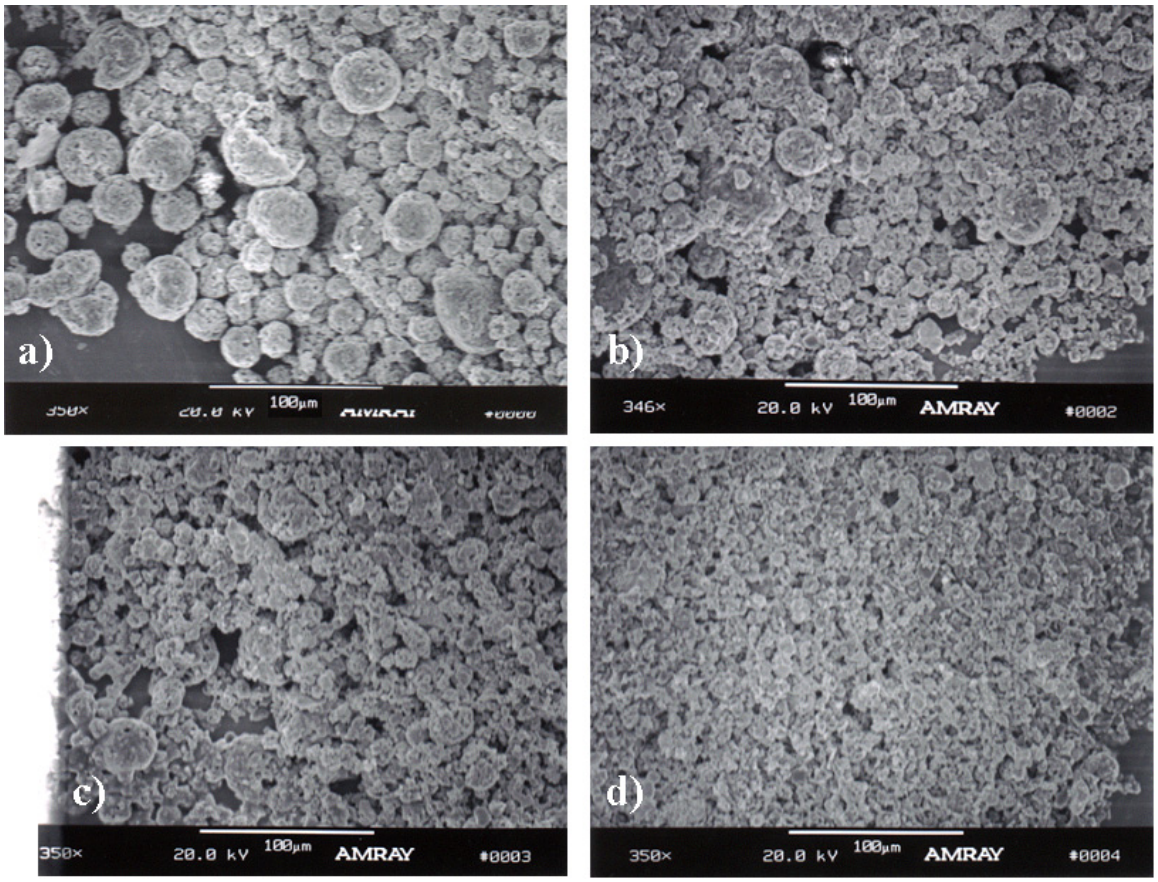

Figure 6: Cermet powder morphology at a) 0.5 hrs, b) 1.0 hrs, c) 2.0 hrs, and d) 16.5 hrs of slurry mixing.

Experimental Design Matrix – DOE III

A statistical design of experiments was created using mixing time (15, 30, 60, 120, 180, and 360 minutes) and pre-wetting the filter paper (pre-wet or not pre-wet), with the standard starting slurry composition (23.5% solids), to create a 6^1 x 2^1 factorial (12 experiments) set of experiments, using 5 repetitions per experiment and two vias per repetition. Those 12 experiments yielded 120 vias for analysis. As in previous analysis, the defect-presence analysis was conducted using maximum-likelihood estimation to estimate values of model parameters and their significance of producing a defect. Modules in Statistical Analysis Software, Proc Catmod and Proc Logistic, were used for analysis on defect formation.[1]

Experimental Procedure - DOE III

The slurry was created in accordance with the work instruction (WI-704191-050 Appendix B) and filling operations followed the same guidelines provided in DOE II above. Slurry mixing was performed with the fitted cover securely on the mixing cup until viscosity measurements were taken and vias were filled. If the experiment called for pre-wetting, filter paper was pre-wet with 250 μl of DGBEA just before via filling was performed.

Statistical Results – DOE III

Neither the paper condition (pre-wet or not pre-wet) nor the mixing time (15-360 minutes) had any significant effect on defect formation. That is, 22% of the samples tested had defects in the as-filled state regardless of these two conditions. It is somewhat surprising that the increased mixing time did not have an effect on defect formation as the corresponding viscosity increase would effect material flow through the via.

Finalized Slurry Filling Criteria

Finalized slurry filling criteria were determined based on three designs of experiments where the following factors were analyzed: vacuum time, solids loading, pressure drop across the filter paper, slurry injection rate, via prewetting, slurry injection angle, filter paper prewetting, and slurry mixing time. Many of these factors did not have an influence on defect formation. In order of decreasing importance, critical factors for defect formation by slurry filling are vacuum time (20 sec. optimal), slurry solids loading (20.0 g of cermet with 13.00 g of DGBEA solvent (21.2 vol%)), filling with the pipette in a vertical position, and faster injection rates (~765 μl/s).

Dome Analysis

From the same ten samples used in Mo homogeneity analysis, dome mass was measured. The cermet slurry domes added to the source feedthru after both vias are filled have two important roles. The first role is to provide a material reservoir to feed the via as the powders consolidate inside the via. This reservoir will allow the filled via to dry as

a solid instead of as a hollow during consolidation. The second role of the domes is to act as a pressure point during the isopressing stage. It has been seen that via compaction is not as uniform without the domes acting to concentrate the pressure onto the cermet instead of the surrounding alumina. Dome mass measurements were needed for computational modeling using GOMA and can be found in Table 3.

Table 3: Cermet Dome Analysis

Dome	Cermet Mass (g)	Corresponding Slurry Mass @ 23.3 vol% (g)	Corresponding Slurry Volume @ 23.3 vol% (ml)
Top	0.153 ± 0.046	0.241	0.119
Bottom	0.116 ± 0.022	0.183	0.091

Technology Transfer to CeramTec

At this point, all via filling with cermet slurry knowledge was passed to CeramTec for use in production. Also transferred was the semi-automated slurry filling apparatus (Figure 7) created to control the following experimental variables; dispensing volume, rate, and tip angle, tip-to-part separation distance, and vacuum time. Ceramtec numbered this assignment Project 3A. The apparatus was used by four operators and was given a fairly good median rating of 7.6 out of 10 with a standard deviation of 2.3. A median of 5 would be equal to the current filling process by hand.

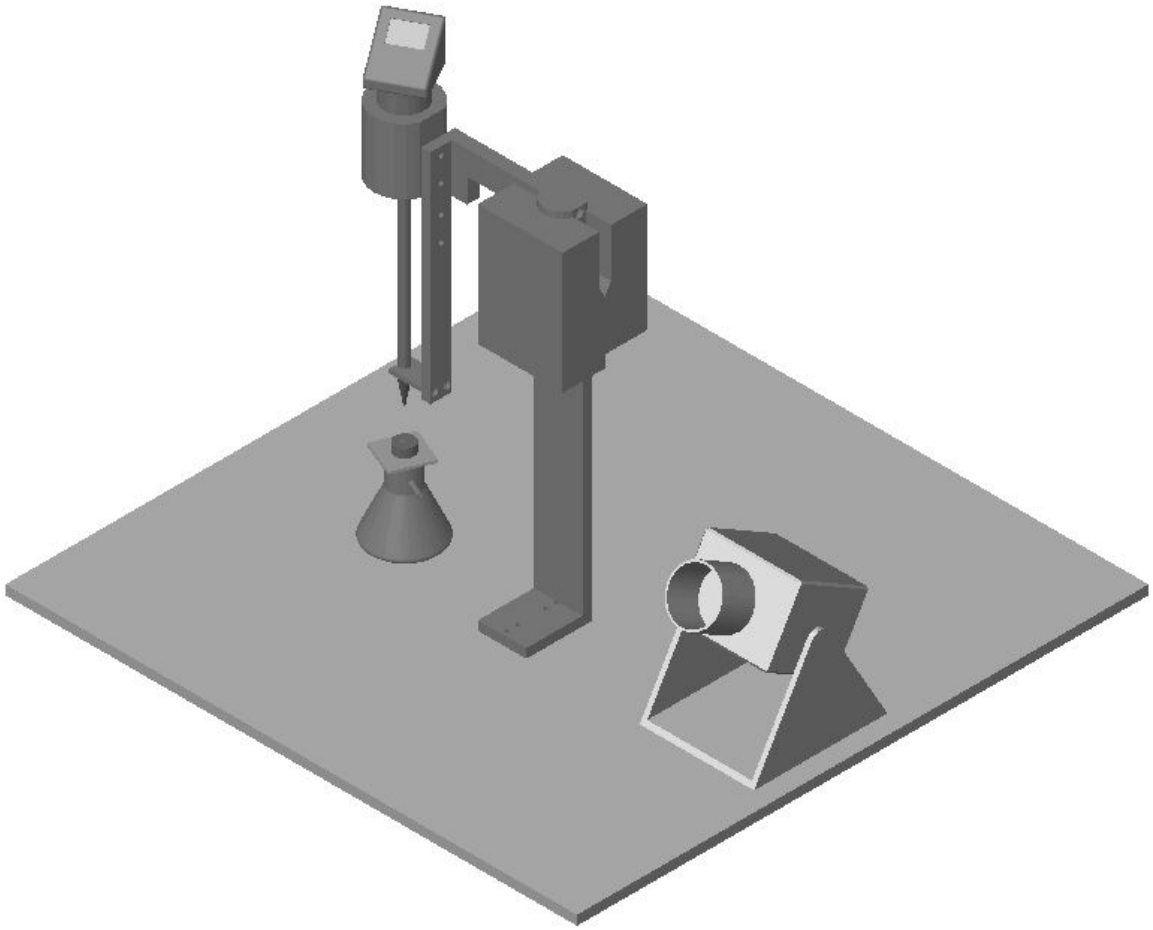

Figure 7: Semi-automated slurry filling apparatus.

6. Viability of High-Solids-Loading-Cermet Paste for Filling Source Feedthru Vias

Paste Preparation Method

A single binder/solvent system was evaluated to asses the viability of high-solids-loading cermet pastes (>40 vol% solids). DGBEA was kept as the solvent strictly for convenience, however the binder system was changed from the insoluble hydroxypropyl methlycellulose/methocel system to a soluble polyvinyl-butyral system (Butvar B79, Soultia). This B79 binder is soluble in DGBEA. The starting powders for pastes were the standard Mo powder, and Sandi94 alumina, which had been calcined to 600°C to remove the existing binders. The starting powders are now nearly equal sized alumina and Mo, which can be easily blended together with a soluble binder and solvent system. With the ultimate goal of creating high-solids-loading pastes, knowledge was drawn from existing high-solids expertise in order to adequately batch and homogenize cermet pastes.

Terry Garino in Sandia's Ceramic Materials Department created the first pastes by batching low solids loading slurries and then evaporating a known amount of solvent by heating. The paste was then three-roll milled. This method worked but was not entirely accurate or easy. Subsequent homogenization and batching was performed by placing batches into containers on an ordinary paint shaker (Red Devil Equipment, Brooklyn Park, MN, USA) for 30 minutes to 1 hour. A few alumina milling media were placed in the containers to aid in the mechanical mixing. The resulting pastes looked homogeneous, possessed no yield stress (they were free flowing), and were much more viscous than the standard cermet slurries. One immediate enhancement over the slurries was seen. Settling times for the pastes were on the order of tens of minutes to several hours as opposed to the 10 to 15 seconds seen in slurries. This added stabilization could only be beneficial in an industrial setting where homogeneity within a batch and between batches is important.

Three-roll milling has a significant effect on rheology of cermet paste (Figure 8). The reason for the decrease in viscosity is most likely due to the breakdown of alumina granules, and homogenization of the alumina/molybdenum/binder suspension. This viscosity reduction is a great benefit to via filling because a higher-solids-loading paste may be able to flow through the via before drying occurs.

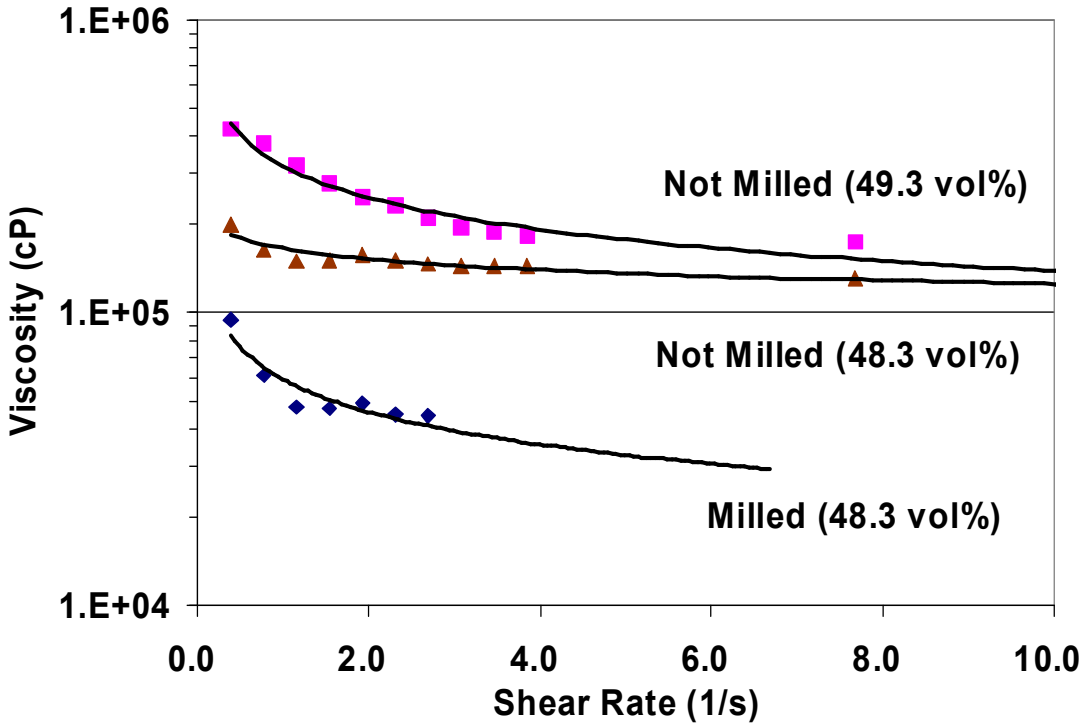

Figure 8: Three-roll-milling effects on viscosity.

Rheology Dependence on Binder

Figure 9 compares the effect of 0.0 to 5.0 wt% B79 binder on viscosity for a 40 vol% paste. From Figure 9, it can be seen that the binder is acting as a dispersant. If there were no dispersing effect added by the binder, viscosity should only increase due to the thickening effect of the dissolved binder in the solvent. However, small additions of B79 actually decrease viscosity over binderless systems (0 wt% dashed line in Figure 9). After an optimal amount of binder is added for dispersion (1.0 wt%), further binder additions increase solvent viscosity and overall viscosity accordingly.

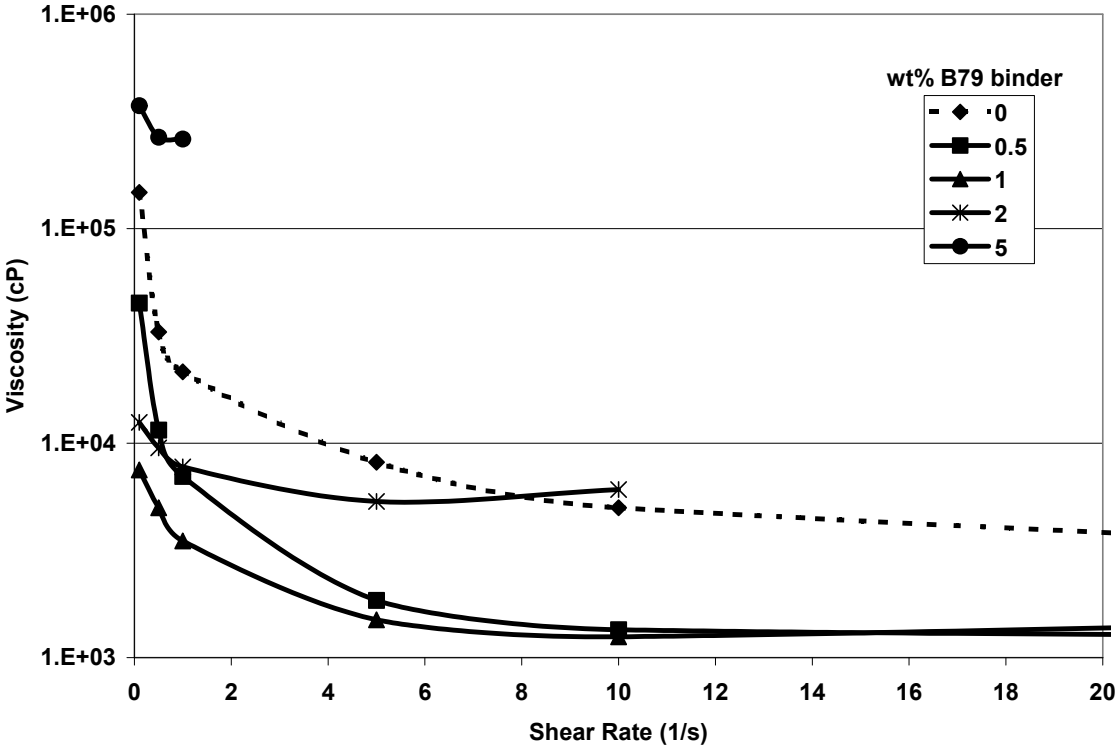

Figure 9: Rheology Dependence on B79 Binder for a 40 vol% cermet paste.

Paste Filling by Hand

As the turbidity of vacuum filling cannot be ideal for defect-free via filling, an alternative method for via filling was explored with high-solids-loading pastes. In this method, the paste was transferred from the mixing container into a disposable syringe and pushed through the via from the large via diameter side. This injectiion was facilitated by a small silicone tube that acted as a gasket between the syringe and alumina blank as shown in Figure 10. The main benefit to this injection method is that the systematic, plug-type-flow of material from one side of the vua to the other entraps less air than vacuum filling. Air is pushed out one side of the via by de-aired slurry coming in from the opposite side.

Figure 10: Schematic of via filling by paste injection.

Ideally, enough material would be inside the via so that the via and surrounding alumina blank will compact in a similar manner, thereby yielding a highly-dense via that meets design specifications for tolerance. Parts that are rejected usually have defects, low-density regions within a via, or are out of specification due to a healed defect (Table 1). It is therefore preferable to fill the via with the greatest amount of material possible, i.e. a highly concentrated paste. Three-roll-milled pastes with solids loadings of 44-50 vol% were created and manually injected into vias.

Filling MC4277 sources with paste that had solids loading greater than 49 vol% were unsuccessful, most likely due to the imbibition that occurs when the paste is in contact with the porous alumina body, thereby increasing the viscosity rapidly (Figure 11) as the paste becomes a solid mass. Only partial fills were obtained with solids loadings greater than 49 vol%. Pastes with 46-48 vol% performed better, allowing complete fills. However, as the solids loading is reduced, a greater amount of shrinking upon drying will occur, which acts as a mechanism for cracking.

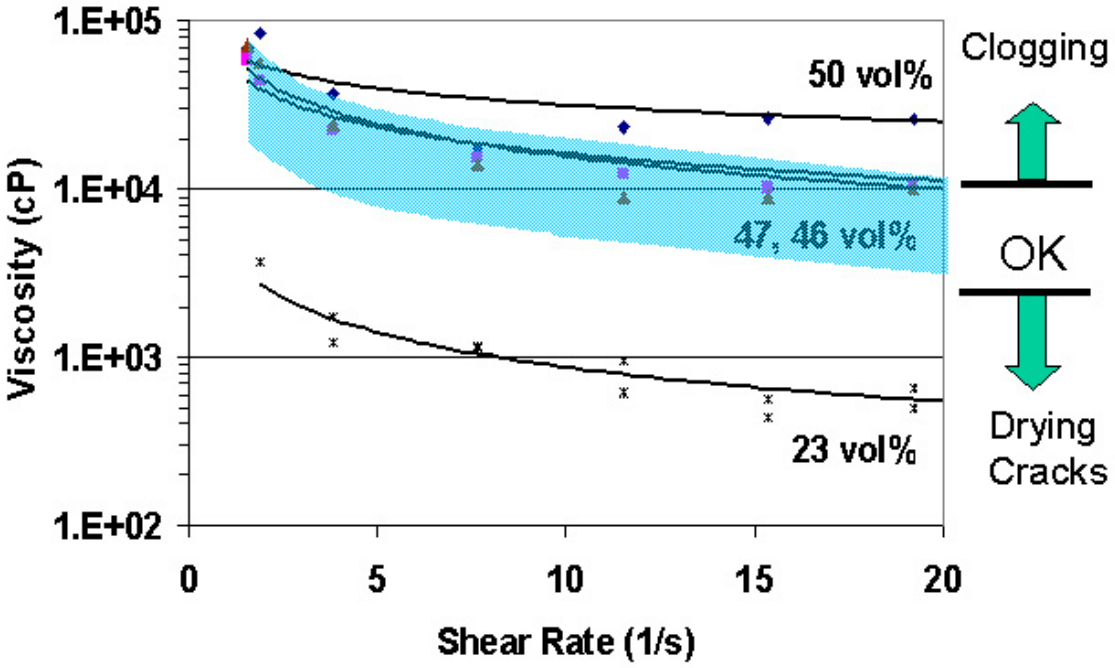

Figure 11: Rheological profiles of three-roll-milled-high-solids-loading pastes compared to low-solids-loading slurry.

The effects of drying cracks on vias filled by 46 and 47 vol% paste can be seen in Figure 12. The 46 vol% paste-filled via had more drying cracks than the 47 vol% paste-filled via. Although all cracks were very small when compared to most slurry-filled vias and were healed during the isopressing step, ideally no defects should be present before isopressing. To further reduce the chance of drying-crack formation, the binder system may need to be optimized further.

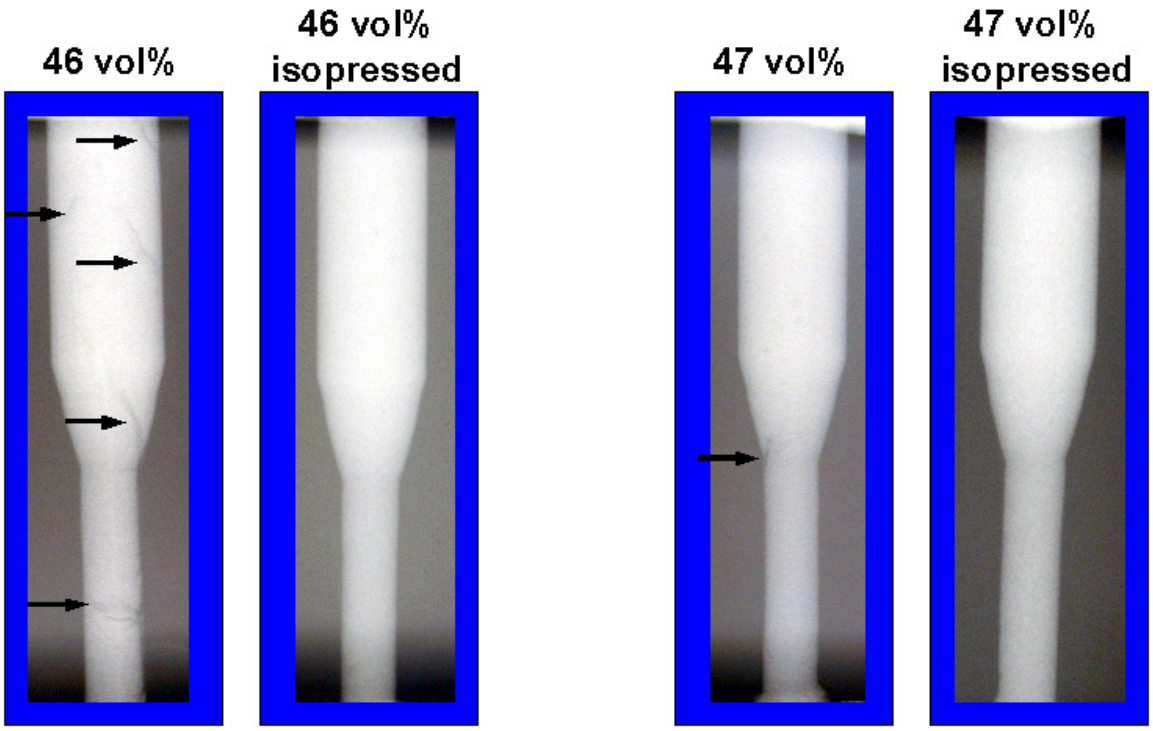

Figure 12: Comparison of as-filled and isopressed vias, filled with 46 and 47 vol% cermet paste.

Paste Filling by Machine

A 48.3 vol% paste was loaded into a stainless steel syringe which was then mounted on a computer-controlled-robotic machine. The machine has the capability to precisely drill vias into an alumina blank, move the part to another station, bring the paste loaded syringe over the via, and inject the via with cermet paste. Control parameters were determined for both via-drilling techniques and via-filling techniques. Figure 13 shows a drilled, filled, isopressed, and fired via made on this machine only after a few iterations. The via drilled by the machine has a slightly modified transition region, well within the confines of the via size and shape specifications. It is thought that this more gradual transition would reduce the chances of defect formation during vacuum filling as many defects were seen in this particular area of the via.

Figure 11 shows the rheological profiles of cermet slurries and pastes. Solvent imbibition into the alumina compact limits the solids loading of cermet pastes that will flow through the via before clogging occurs. It is preferable to have as high a solids loading paste as possible that does not clog. If the solids loading is too low, drying

cracks occur similar to those formed with standard cermet slurry without vacuum assisted consolidation. In Figure 11, the acceptable range of rheological profiles (adjusted by solids loading) for non-vacuum assisted filling is outlined.

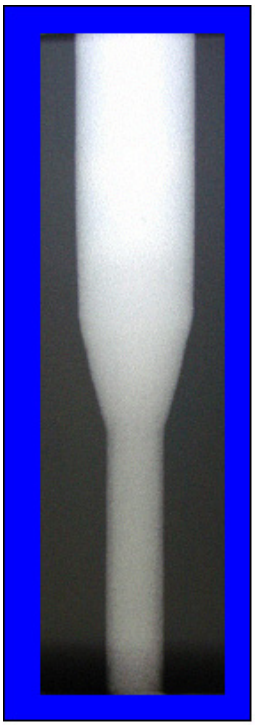

Figure 13: Source feedthru filled by machine and 48.3 vol% paste.

Paste Filling at CeramTec

Slurry-fill operators at CeramTec were given a 42 vol% solids loading cermet paste and a 10 cc glass syringe with silicone tubing gasket. One operator filled twenty parts (10 dry and 10 pre-wet with 100 μl of solvent) after a few minutes of instruction according to CeramTec's Project 3B. Results of those tests were positive with the conclusions as follows:

Analysis before isopressing:

"From this limited test it appears that there is no advantage in pre-wetting vias prior to filling. Paste filling does appear to be an acceptable method for via filling. The results from the pre isopressed parts is better than noticed in parts filled by the traditional slurry method. Paste filling should be given further consideration."

Analysis of filled and fired parts after cross sectioning:

"Paste filling could be a viable option to slurry filling. There was, as expected, less shrinkage of paste filled vias than the standard slurry method. The underfilled condition frequently seen in slurry filled parts was not seen in the paste filled parts in the project. However it does appear that large pockets of air are trapped in the paste filled parts which caused the large voids seen. If this assumption is correct some method of removing air prior to filling could greatly improve the integrity of the via. Some automation to the paste filling process would be preferred over hand filling. I would expect applying a controlled pressure to the paste during filling would be advantageous."

Further analysis to the cause of the 'large pockets of air' trapped in the via showed that the violent mixing action due to paint shaking introduced bubbles into the system. It was found that slow rolling of the paste for approximately eight hours was enough to de-air the slurry and produce defect-free vias.

Paste Filling MC4300 'Doglegs'

A new source feedthru design was filled using 40 vol% cermet paste. The paste was batched on a paint shaker with 1.5 wt% B79 binder. Only a single iteration was needed to obtain complete fills of this new source feedthru, the result of which is seen in Figure 14.

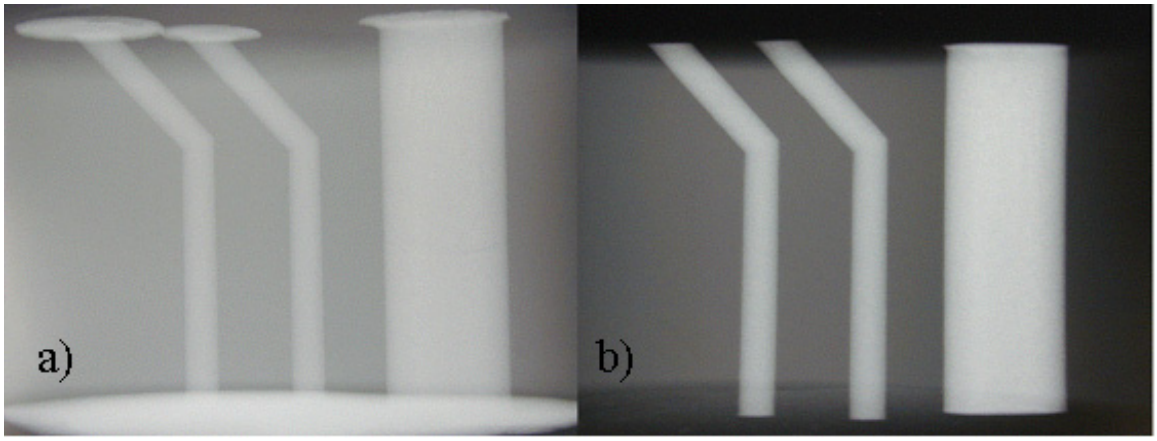

Figure 14: Paste-filled MC4300 source feedthru, isopressed a) and fired b).

Paste Filling Conclusions

The paste-filling process is easy to implement and easier to use when implemented. Higher yields may be achieved due to the robust nature of the process, however a more in depth study may be needed for validation. However, from the fair number of samples already filled, the likelihood of this process being a viable and reliable process is very good. Issues of concern for the paste process are any problems that may arise in subsequent manufacturing stages into the neutron tube. Microstructure characterization later in this report will help to ensure that changes in microstructure are quantified and related to variability seen in fabrication processes.

7. Optimize CND50

Powder Preparation Methods

As mentioned previously, Sandia Laboratories and CeramTec use very different ball-milling setups to mill Sandi94 alumina and Mo powder together. Larger batch sizes, different milling speeds, and differences in media sizes can all lead to different powder morphologies and thus differences in compaction behavior as well as powder flow and die filling. Cermet powders of 0.5, 1, 4, and 20 hours were ball milled using the standard Sandia ball milling setup and batch size. Spray-dried cermet granules from the non-aqueous-spray dryer at Niro and mist-granulated granules were also investigated for compaction behavior on a powder-testing center (PTC) (KZK Powder Tech Corp, Chantilly, VA, USA)

A right-circular cylinder made of cermet was needed for triaxially measuring dimensions during isopressing. The cermet cylinder had to be strong enough to experience moderate handling while preserving the original powder morphology. It was determined that a cylinder created at 1000 psi would yield enough information during tri-axial testing to model the compaction behavior because as most of the compaction occurs below 10000 psi. Cermet powder dry-ball milled 4 hours and isopressed to 1000 psi proved difficult to chuck horizontally in a lathe (to mimic standard methods of green machining cermet). Freeze drying into a metal mold 1.75” diameter and 3.5” tall yielded a non-perfect cylinder. Therefore, a right-circular cylinder was obtained using a slug of cermet powder isopressed to 1000 psi and mounted in an epoxy base. The epoxy base

was easily chucked in a mill and a right circular cylinder was milled using diamond tooling. The cermet cylinder was then fit with strain gauges, two located orthogonal at the middle of the sample and one located along the long axis.

Powder Characteristics

In addition to compaction behavior, angle of repose and die-fill density play an important role in the production of pressed cermet parts. Die-fill density and angle of repose for several cermet systems can be found in Table 4. There were no significant differences seen in die-fill density, a measure of how well the powder fills the cavity. Ewsuk et al should be referenced for a detailed background on cermet compaction.[4-6] However, the angle of repose shows a large variation in flow behavior of samples in Table 4. The larger, spray-dried Sandi94 primary granules, which are used for compact fabrication, have a much lower angle of repose (29°) indicating excellent flow behavior. Secondary spray-dried Sandi94 granules are used in the CND50 blending process and show a relatively poor angle of repose of 79°. When combined with Mo powder (angle of repose of 92° - an overhang) in the dry blending process for 4 hours, an even poorer flow behavior (89°) is achieved. Standard-blend CND50 essentially does not flow on its own outside of mechanical influence such as vibrations which are needed to induce powder flow.

The purpose of spray-drying cermet was to create an intimately mixed, flowable powder. The ethanol/toluene (40/60 by weight) based slurries used in the nitrogen-atmosphere-spray dryer at Niro were created with approximately the same volume-binder content as the conventionally-spray-dried Sandi94 so that green machining characteristics might be compared more easily. Batch calculations for the three binder systems can be found in Table 5. Spray-dried cermet granules show poor flow characteristics as well, with angles of repose of 68-78°. The reason for the poor flow characteristics can be deduced from SEM micrographs of the granules in Figure 15-Figure 17 where small particulates are scattered among the larger, spray-dried granules. These small particulates, or fines, are common in small batch spray dryers, such as the one used at Niro for these particular batches, and hinder flow of the granulated powder. Flow properties of these granules could be improved by sieving out the fines.

One of the first attempts at mist granulating cermet with B79 binder shows a promising 28° angle of repose. Figure 18 shows the atomization of cermet slurry from the ultrasonic tip during the mist granulation process. The SEM micrograph in Figure 19 shows spherical granules and no fines created from mist granulating a 17 vol% slurry with 0.5 wt% binder. These granules have a low bulk density because they were created from a low-density slurry. In mist granulation, the granules will have approximately the same density as the slurry solids loading due to the sublimation process. Spray-dried granules undergo shrinkage during the drying stage, making the final-granule density a function of the spray dryer conditions such as humidity. It may therefore be possible to easily tailor starting-granule density by simply changing the solids loading of the slurry in the mist granulation process. Conceivable limitations of this procedure though are difficulty in obtaining high-granule densities, which require high-solids-loading slurries that may not be able to be granulated by the ultrasonic horn due to high viscosities. In this case, the consolidation, and thus partial densification, of the granule during spray drying would be more appropriate.

Table 4: Cermet Powder Characteristics

Sample	Fill Density (% theoretical)	Angle of Repose (deg)
Sandi94 alumina primary*	22.3	29
Sandi94 alumina secondary*	22.8	74
Mo powder	25.1	92
0.5 hr DBM CND50+	24.0	88
1 hr DBM CND50+	23.4	77
4 hr DBM CND50+	20.7	89
20 hr DBM CND50+	22.8	88
SD with B79 binder*	16.3	78
SD with Ethocel binder*	24.3	68
SD with Klucel E binder*	22.5	69
MG with B79 binder×	10.3	28

∗ Spray-Dried Powder
+ Dry-Ball-Milled Powder
× Mist-Granulated Powder

Table 5: Slurry Compositions for Non-Aqueous-Spray-Dried Cermet.

	B79 Batch (polyvinyl butyral)		Ethocel Batch (ethylcellulose)		Klucel E Batch (hydroxypropylcellulose)	
	wt (g)	vol %	wt (g)	vol %	wt (g)	vol %
40/60 (by wt.) Ethanol/Toluene	7564.5	61.7	7500	65.9	7500	66.2
Binder	441.1	3.6	400	2.9	400	2.9
Dibutyl Pthalate (plasticizer)	22.06	0.17	80	0.56	60	0.42
Dispersant	227	1.64	179	1.16	134	0.87
Calcined Sandi94	11020	23.8	11020	21.3	11020	21.4
Mo	11360	9.1	11360	8.1	11360	8.2
Total Solids Loading		38.3		34.1		33.8

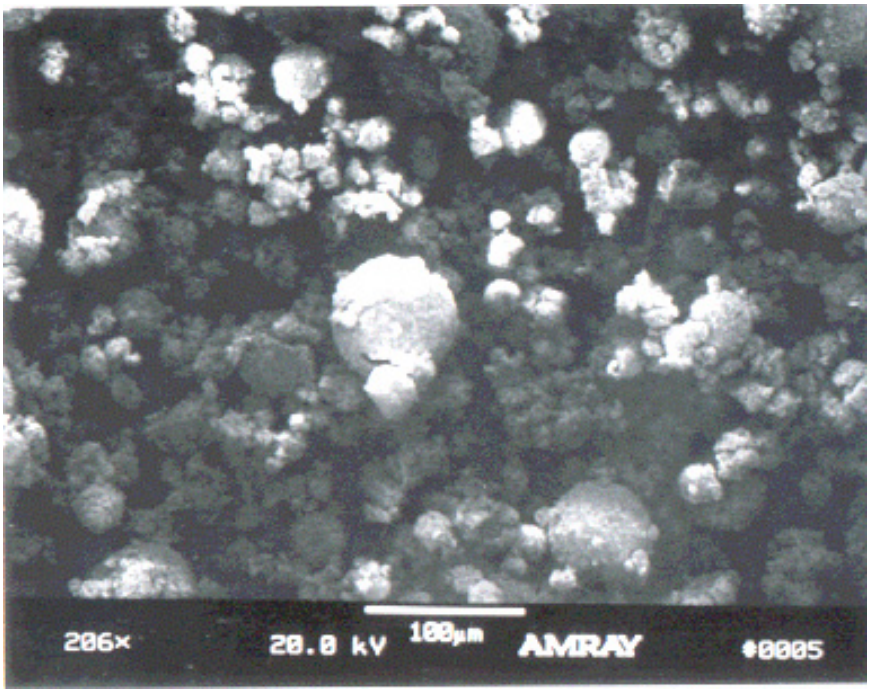

Figure 15: Spray-dried cermet with B79 binder.

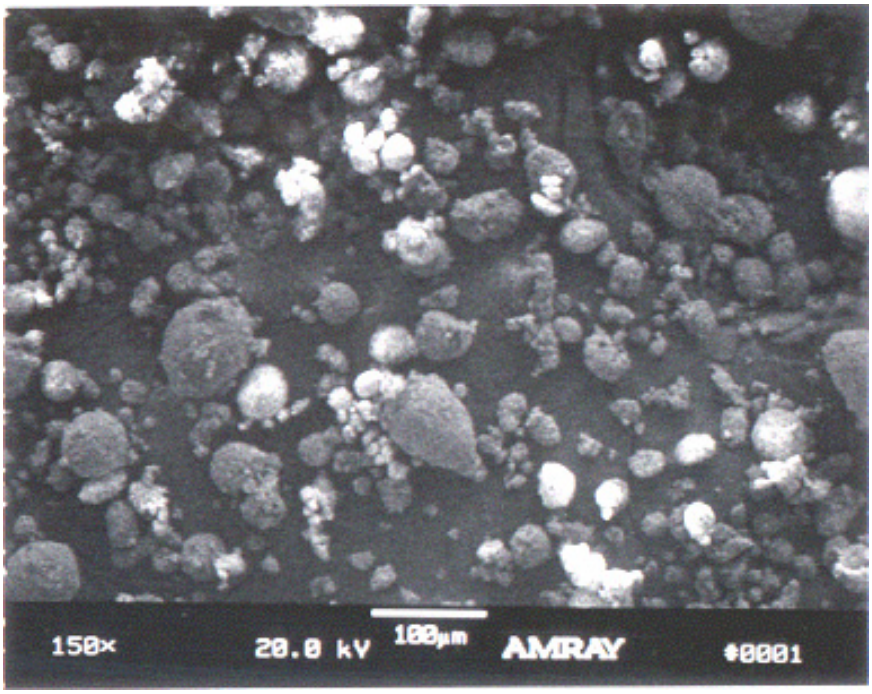

Figure 16: Spray-dried cermet with Ethocel binder.

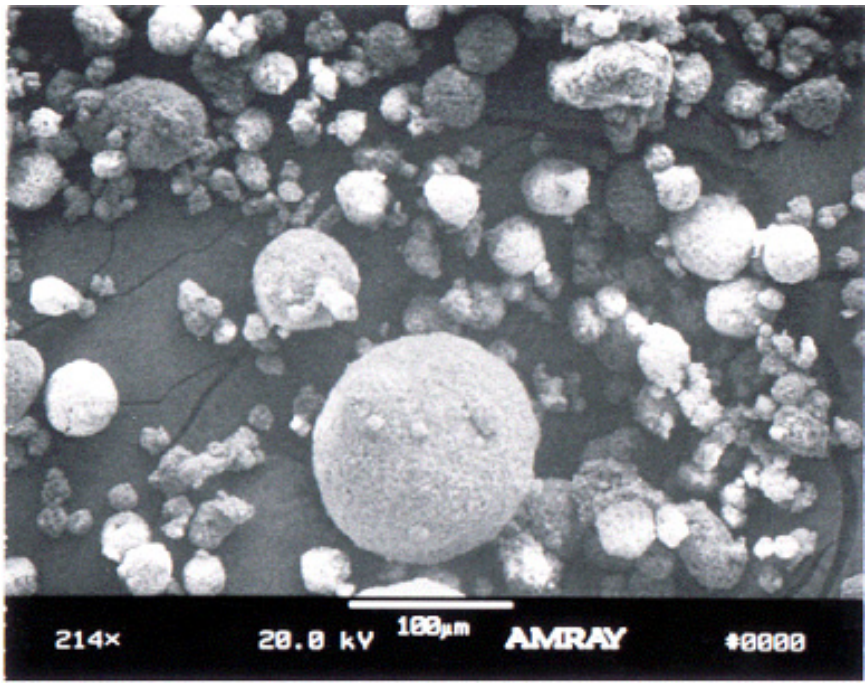

Figure 17: Spray-dried cermet with Klucel E binder.

Figure 18: Mist granulation of cermet slurry through an ultrasonic horn.

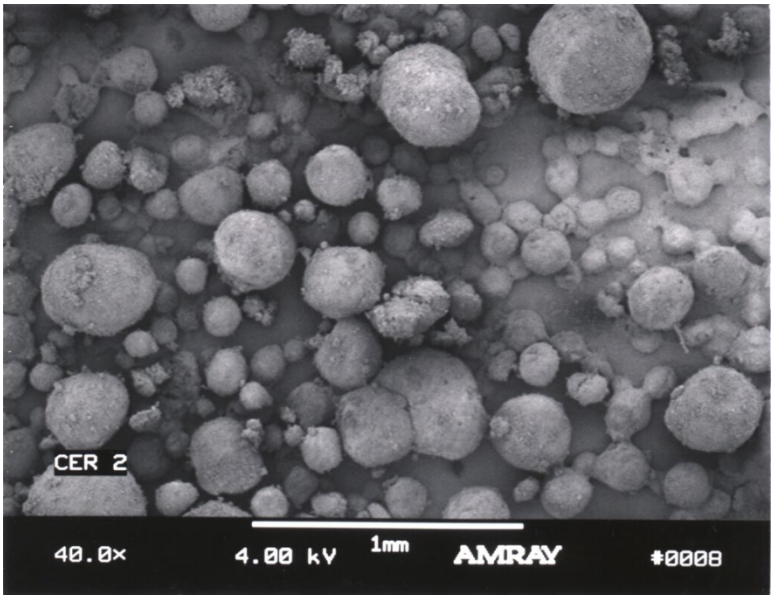

Figure 19: Mist-granulated cermet with B79 binder.

Compaction Analysis

Compaction curves of each powder listed in Table 4 were obtained by pressing to 55% of theoretical density. Important features in each curve is the theoretical density at low pressures (an indication of die filling density), the slope of the curve (an indication of granule deformation mechanics), and pressure required to reach 55% theoretical density (how well the powder compacts). There are many more aspects to compaction that could be analyzed to gain more insight into how well each powder compacts, however, this study will focus more on the comparative compaction behaviors of each system and less on the detailed analysis of cermet compaction behavior.

Figure 20 compares the compaction behavior of the basic constituents of cermet; Sandi94-s (secondary granules or fines) and Mo to the standard CND50 (4 hour DBM). The benefits of granulation can be seen in the shallow slope of the Sandi94-s compaction curve when compared to the steep slope of pure Mo powder. Further, the Sandi94-s reaches 55% density at a lower compaction pressures, indicating better granule deformation and powder mobility.

Figure 21 compares cermet powders dry-ball milled at 0.5, 1.0, 4.0, and 20.0 hours. The 20.0-hour sample does not show good compaction behavior whereas the 0.5, 1.0 and 4.0-hour samples are more ideal. A small change in compaction density (20.0 hour sample) promotes the presence of compaction voids as material movement is decreased as compared to larger changes in compaction density (0.5, 1.0, and 4.0 hours samples). This small change in compact density, in addition to the decreased dispersion of molybdenum in the 20.0-hour sample, may help explain the poor machining characteristics of this powder.

Figure 22 compares spray-dried powders produced from non-aqueous-spray drying at Niro. A qualitative assessment from CeramTec deemed the Ethocel system better than the B79 and Klucel E systems for green machining. There is no discernable difference in the compaction curves in these three systems. The green machining characteristics are therefore attributed to the material properties of the binder itself.

Figure 23 compares the optimal granulated powders from each granulation method; spray drying, mist granulating, and ball milling. A very good performing granulated powder, Sandi94-p, is also included in Figure 23 for comparison. Ball-milled

powder (CND50) shows a high fill density and a shallow compaction curve as compared to Sandi94-p, whereas mist-granulated and spray-dried cermet have more comparable fill densities and similarly-shaped compaction curves. It is interesting to note that higher compaction densities are achieved with mist-granulated and spray-dried powders at pressing pressures greater than ~2000 psi as compared to ball-milled powder, suggesting higher strength compacts and greater sintered densities are possible.

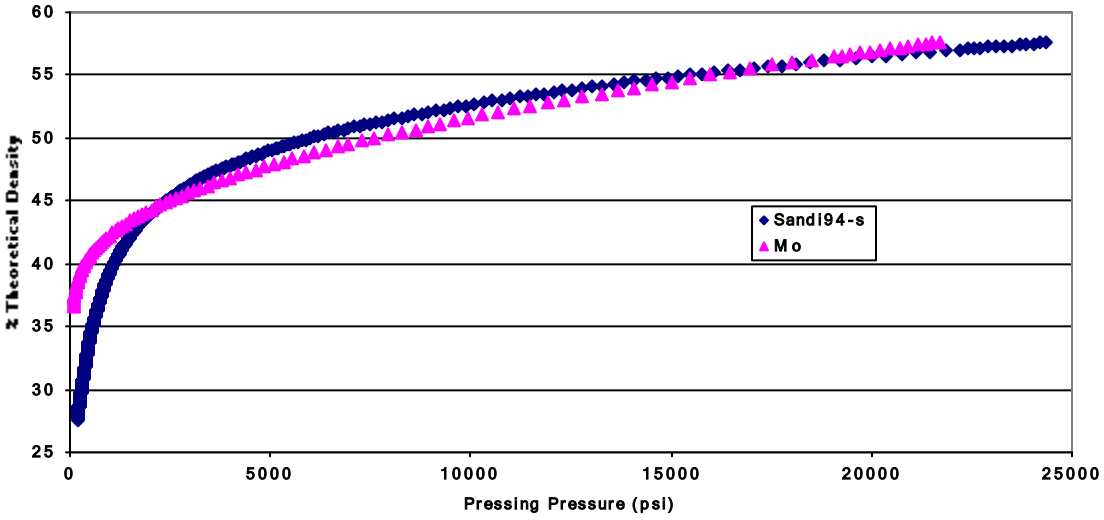

Figure 20: Compaction behavior of spray-dried Sandi94-s and Mo powder.

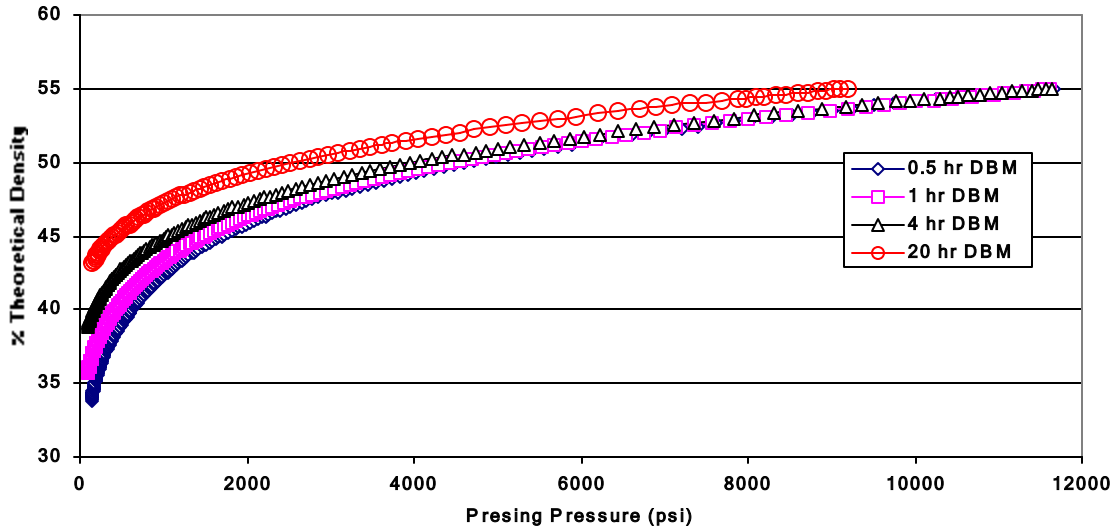

Figure 21: Compaction behavior of dry-ball-milled CND50.

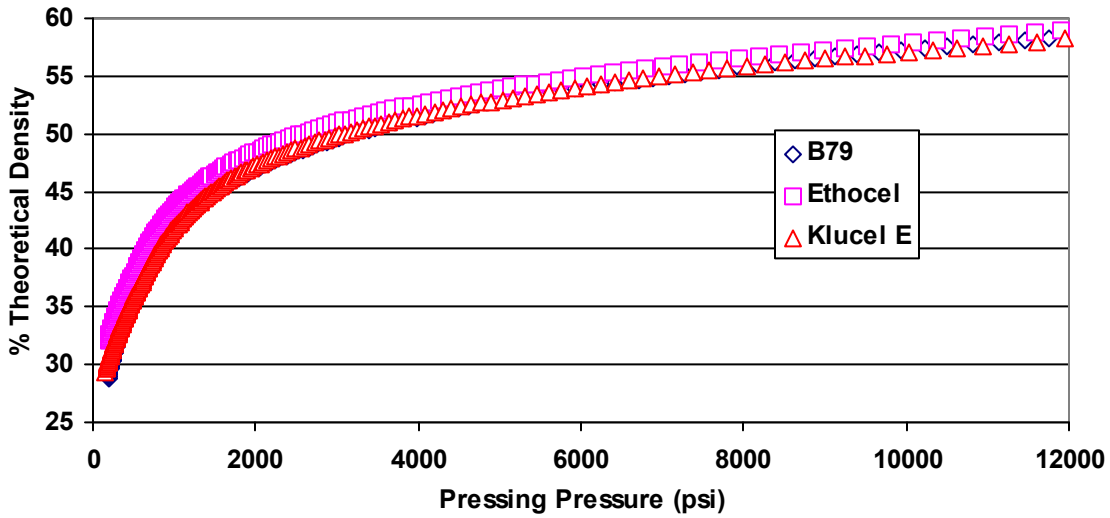

Figure 22: Compaction behavior of non-aqueous-spray-dried cermet.

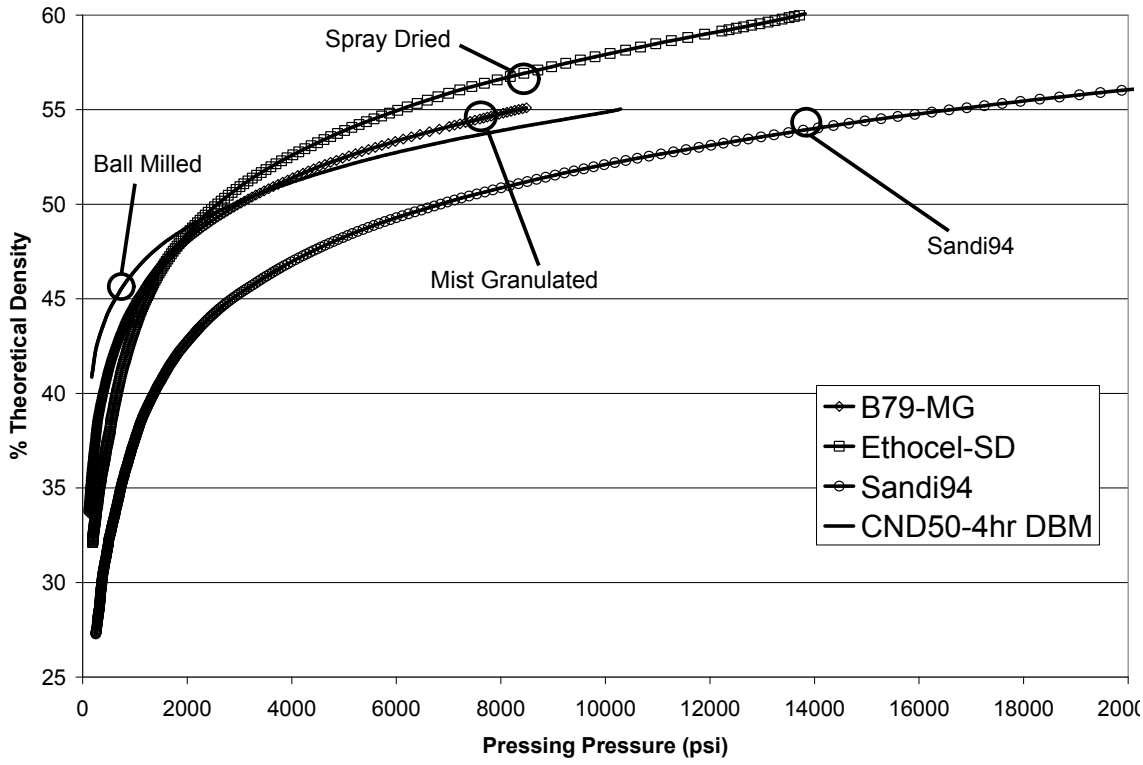

Figure 23: Compaction behavior of cermet mist-granulated with B79, spray-dried with Ethocel, spray dried Sandi94-p, and 4hr dry-ball-milled.

Tri-Axial Testing Results

Figure 24 shows the tri-axial compression test data of the right circular cermet cylinder machined from a 1000 psi compressed slug. Data from one of the two axial gauges is missing, possibly due to a bad strain gauge. At approximately 7000 psi, the other axial strain gauge slips, causing a step in the data. At approximately 11000 psi, both strain gauges slip and the remainder of the data is lost. Reliable data shows that a greater displacement is seen axially as opposed to laterally, which is normal. Retesting could not be completed due to lack of resources and thus, compaction modeling could not be applied to this data. However, if the above fabrication steps are followed, the right-circular cylinder of cermet should be relatively easy to recreate.

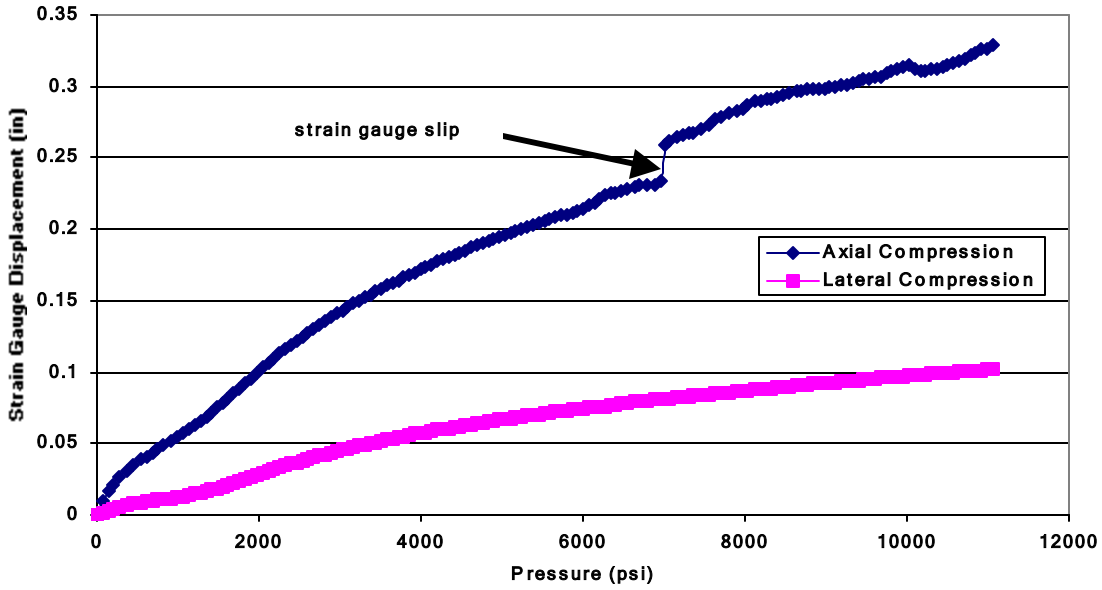

Figure 24: Tri-axial testing of 4 hour DBM cermet right-circular cylinder.

8. Microstructure Characterization by Tessellation

Background

In order to understand the influence of changing processing conditions on any cermet microstructure, a microstructure characterization procedure needed to be developed so that direct comparisons could be made. Several indispensable resources at Sandia National Laboratories were used to initiate the microstructure characterization technique used in this study.[7-8] Tessellation is a common method of analyzing a single phase in a binary phase microstructure. An example of a tessellated microstructure image can be seen in Figure 25. In cermet microstructures it is advantageous to analyze the conducting Mo phase as it is the lesser phase by volume (~27 %) and dominates several aspects of cermet performance such as conductivity, thermal strain, and machinability. Tessellation isolates the selected phase (Mo), draws a border around the isolated islands of this phase, removes the secondary phase Al_2O_3, and expands these borders simultaneously until all empty space is filled, forming a single-phase microstructure. From this single-phase microstructure, various algorithms can be created to understand how dispersed the Mo particles are, how homogeneous the dispersion is, and how 'string-

like' the Mo particles are. Each of these three features of the Mo microstructure can be related to actual physical properties of interest.

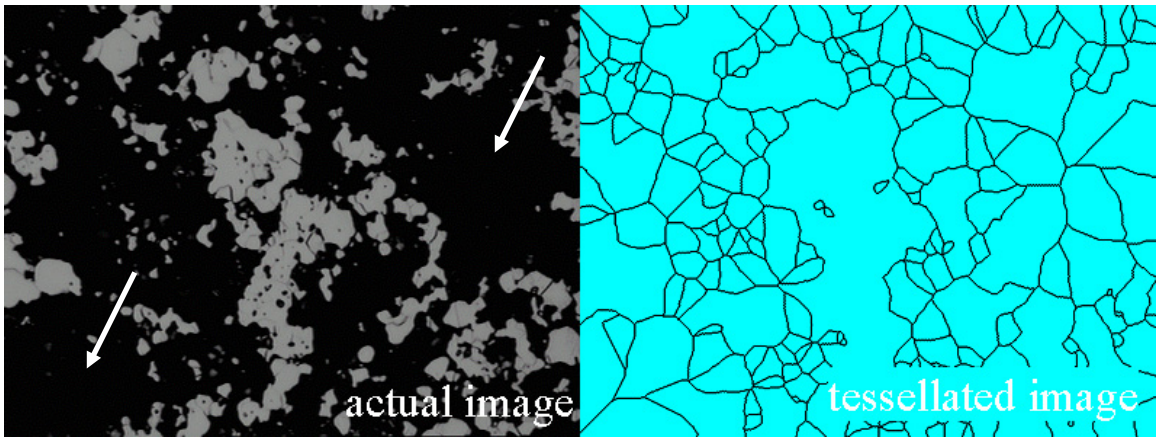

Figure 25: Example of tessellating an image (4 hr DBM sample) with arrows pointing to areas void of .

Dispersion

Mo particle size for standard Sandia cermet processing ranges from 4-8 μm based on mass with a relatively narrow distribution. This mass distribution of 4-8 μm translates to an average particle size of 2.3 μm for a particle number distribution. Various processing conditions may effectively change the Mo particle size by causing the Mo particles to agglomerate together. Although these particles are not physically joined together on the atomic level, their extremely close proximity creates more areas in the cermet that are void of the conducting phase (arrows Figure 25). Dispersion is depicted in Figure 26a and b.

It should be noted that most particle size analysis data is outputted in the form of mass distribution of particles of specific size ranges. In this study, the number distribution of particles is required because it is the number of particles in each image being counted and calculated. If the mass distribution is used in the analysis, artificially high dispersion values will arise due to the shift to greater average particle size caused by higher mass particles.

In Equation 1, the algorithm used to describe a tessellated microstructure in terms of Mo dispersion compares the number of tessellated cells that should theoretically arise

if perfect dispersion (of same-sized Mo particles) occurs to the actual number of tessellated cells formed by the microstructure. The average cross sectional area is calculated based on ¼ the average particle diameter since, statistically, a Mo particle will not be cross-sectioned on its diameter, but ¼ of its diameter.

Equation 1: Algorithm Describing Microstructure Dispersion

$$\text{Dispersion Index (DI)} = \frac{\text{Actual \# of Tessellated Cells (ATC)}}{\text{Theoretical \# of Tessellated Cells (TTC)}} * \text{Vol Fraction Mo}$$

where

$$\text{TTC} = \#\text{ of Mo Particles} = \frac{\text{Actual Area of Mo}}{\text{theoretcial particle area} \big/ \text{particle}}$$

where

$$\text{theoretcial particle area} = \frac{3}{4}\pi\left(\frac{\text{particle diameter}}{2}\right)^2$$

therefore

as $\text{DI} \Rightarrow 1$: more dispersed

as $\text{DI} \Rightarrow 0$: more coalesced

As the ratio of the number actual tessellated cells to the number of theoretical tessellated cells approaches one, the microstructure becomes more dispersed. This ratio will be referred to as the dispersion index (DI) with numbers approaching zero indicating poor dispersion and number approaching one indicating good dispersion.

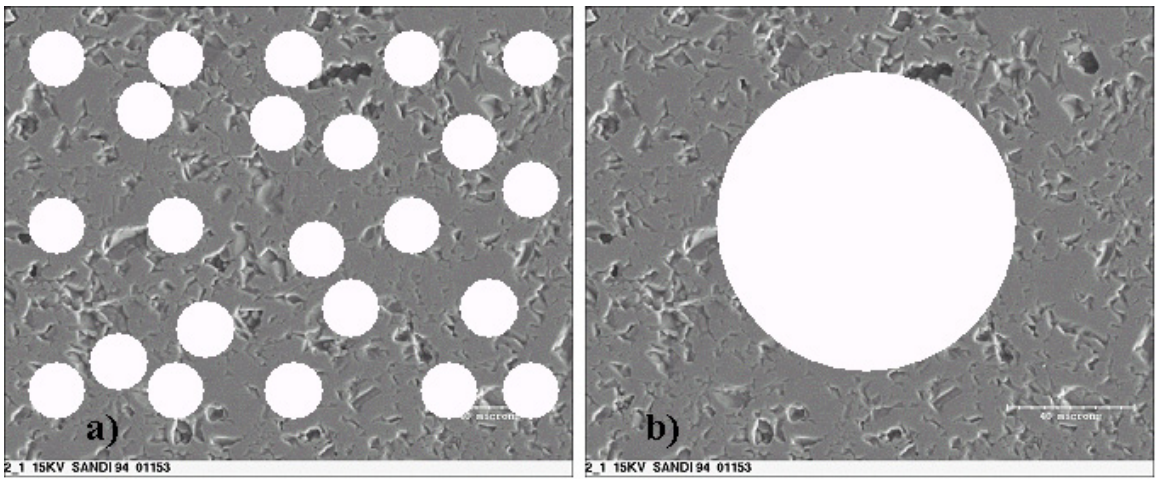

Figure 26: a) Schematic showing fully dispersed Mo particles and b) all particles agglomerated.

Homogeneity

Dispersion alone is not enough to fully characterize the Mo particles in the microstructure, it is important to also numerically describe how the Mo particles are located with respect to one another. Homogeneity is a way to describe how random or ordered the Mo phase is within the surrounding Al_2O_3. A schematic of a homogeneous and relatively inhomogeneous Mo phase distribution can be found in Figure 27. A perfectly homogeneous distribution of particle in three dimensions is analogous to a face-centered-cubic lattice of atoms. Tessellated cells of a perfectly homogeneous distribution of particles would have a hexagonally shaped cross section with a longest dimension defined as **2x** in Equation 2. Variations in the measured longest dimension of an actual tessellated cermet microstructure are deviations from the perfectly homogeneous case. The ratio of the theoretical maximum dimension to the standard deviation of measured maximum dimensions is the homogeneity index (HI).

Equation 2: Algorithm Describing Microstructure Homogeneity

$$\text{Homogeneity Index (HI)} = \frac{\text{Theoretical Maximum Dimension}}{\sigma_{\text{measured maximum dimension of tessellated cells}}}$$

where

$$\text{Theoretical area of a cell is } A_0 = \frac{\text{Total Area Measured}}{\#\text{ of Cells Measured}}$$

and

$$A_0 = \frac{3\sqrt{3}}{2}x^2$$

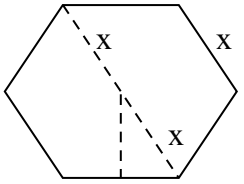

where 2x is the Theoretical Maximum Dimension

therefore

as $DI \Rightarrow 1$: more dispersed

as $DI \Rightarrow 0$: more coalesced

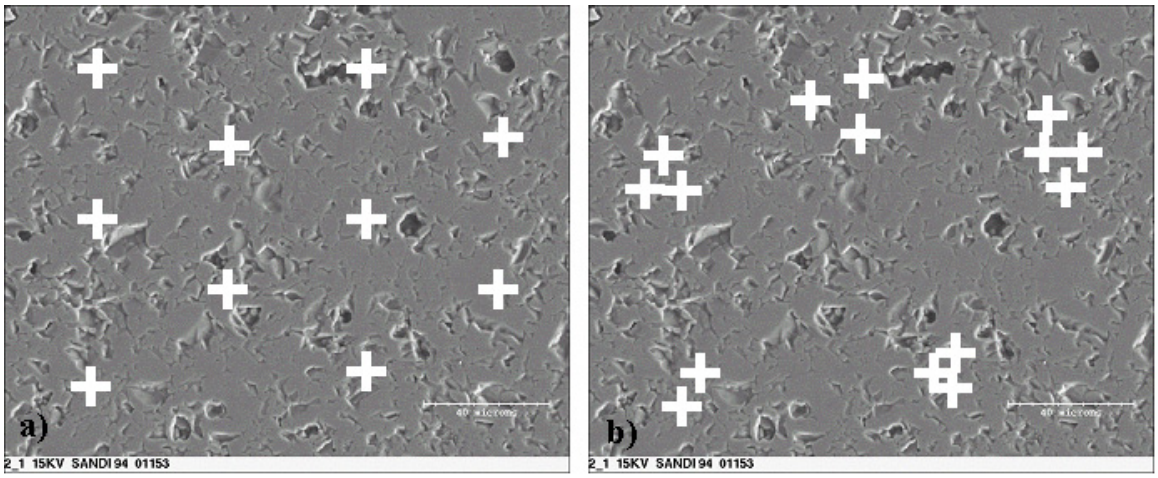

Figure 27: Schematic comparing a homogeneous microstructure a) to an inhomogeneous microstructure b).

Percolation

One critical function of cermet is to conduct electricity. In an ideal case, there would be a small amount of Mo in the cermet microstructure to reduce stresses created by thermal expansion mismatch between the Mo and Al_2O_3, yet still enough Mo to provide a conductive pathway for electrons. For the theoretical case of monodisperse spheres, approximately 17 vol% is necessary to form a percolating pathway. In practice, it is safer to have excess conducting phase to ensure a conductive pathway will occur. For cermet processing approximately 27 vol% Mo is used. In order to ensure alternative processing methods do not upset the amount of percolating pathways found in standard cermet microstructures, a percolation index (PI) was defined by examining the 'stringy-ness' of the tessellated cells. If Mo particles form long, string-like, chains that are analogous to wires, it is more likely a percolating network will form. These string-like agglomerated Mo particles will form string-like tessellated cells as seen in Figure 28. The algorithm used to describe the shape of the Mo particles is given in Equation 3. For any given area, the shortest perimeter around that area is a circle. The greater the perimeter, the less circular and more string-like the area becomes. For cermet microstructures, the perimeter for each tessellated cell is compared to the perimeter that would theoretically bound each cell area to a circle.

Further, if the particle is particularly large, it will have a higher tendency to percolate, so a factor is included in the calculation to account for this. Also, if there is a

large volume fraction of conducting phase in the microstructure, there will be a higher tendency to percolate, so a factor taking into account the the volume fraction of conducting phase is also included in the calculation. In general, larger values for PI indicate a greater likelihood to percolate.

Equation 3: Algorithm Describing Microstructure Percolation

$$\text{Percolation Index (P.I.)} = \mathrm{M}_0 \times \left[avg\left(\frac{\text{actual perimeter of tess. cell}}{\text{theoretical perimeter of tess. cell}} \times \frac{\text{tess. cell area}}{\text{avg cell area}} \right) \right]$$

where

$\mathrm{M}_0 = \text{volume fraction of Mo}$

$$\text{Theoretical Circular Perimeter} = 2\pi \sqrt{\frac{\text{measured area}}{\pi}}$$

therefore

$\text{as DI} \Rightarrow 1 : \text{more dispersed}$

$\text{as DI} \Rightarrow 0 : \text{more coalesced}$

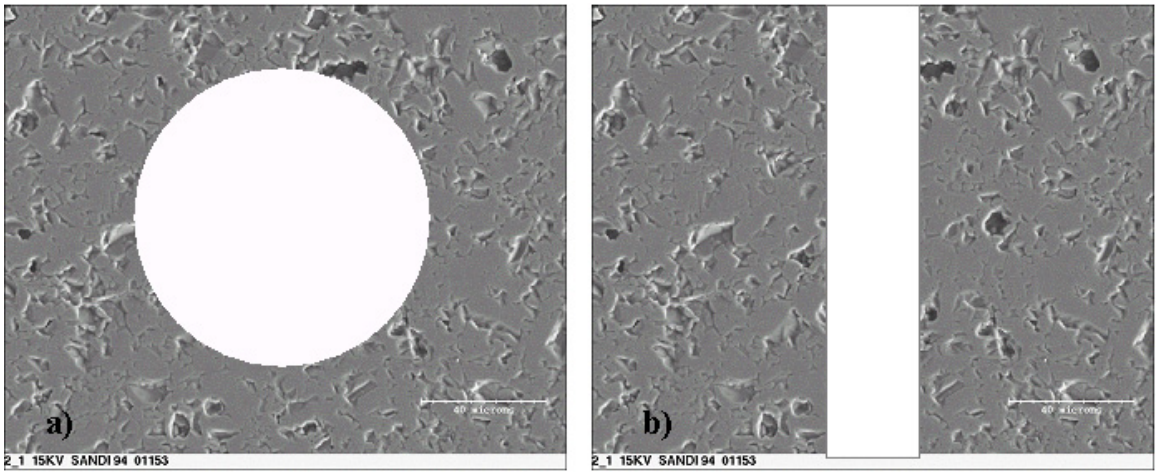

Figure 28: Schematic comparing a non-percolating Mo phase network a) to a percolating network b).

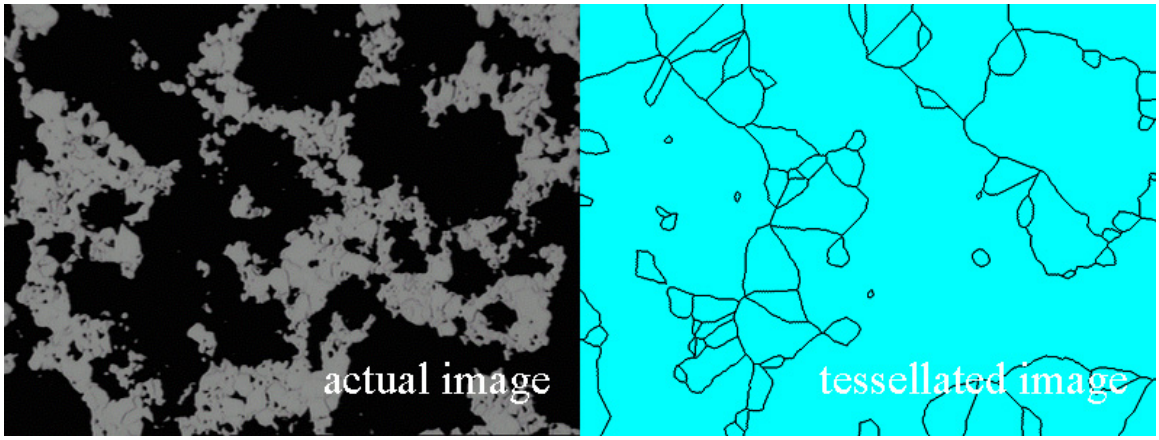

Figure 29: Example of string-like agglomerations of Mo forming a string-like tessellated image (20 hr DBM).

Combining Dispersion, Homogeneity, and Percolation

It is well known for structural composites that a homogeneous dispersion of the strengthening particulate phase provides the highest overall composite strength. Therefore, these structural composites would have high dispersion and homogeneity indices. However, in this configuration, the strengthening particulates are perfectly isolated from each other, making electrical conductivity impossible. On the contrary, if the secondary phase is long and string-like in the composite, mechanical strength is compromised for a percolating network. This idea is depicted in Figure 30 where dispersion, homogeneity, and percolation indices are plotted on the same graph.

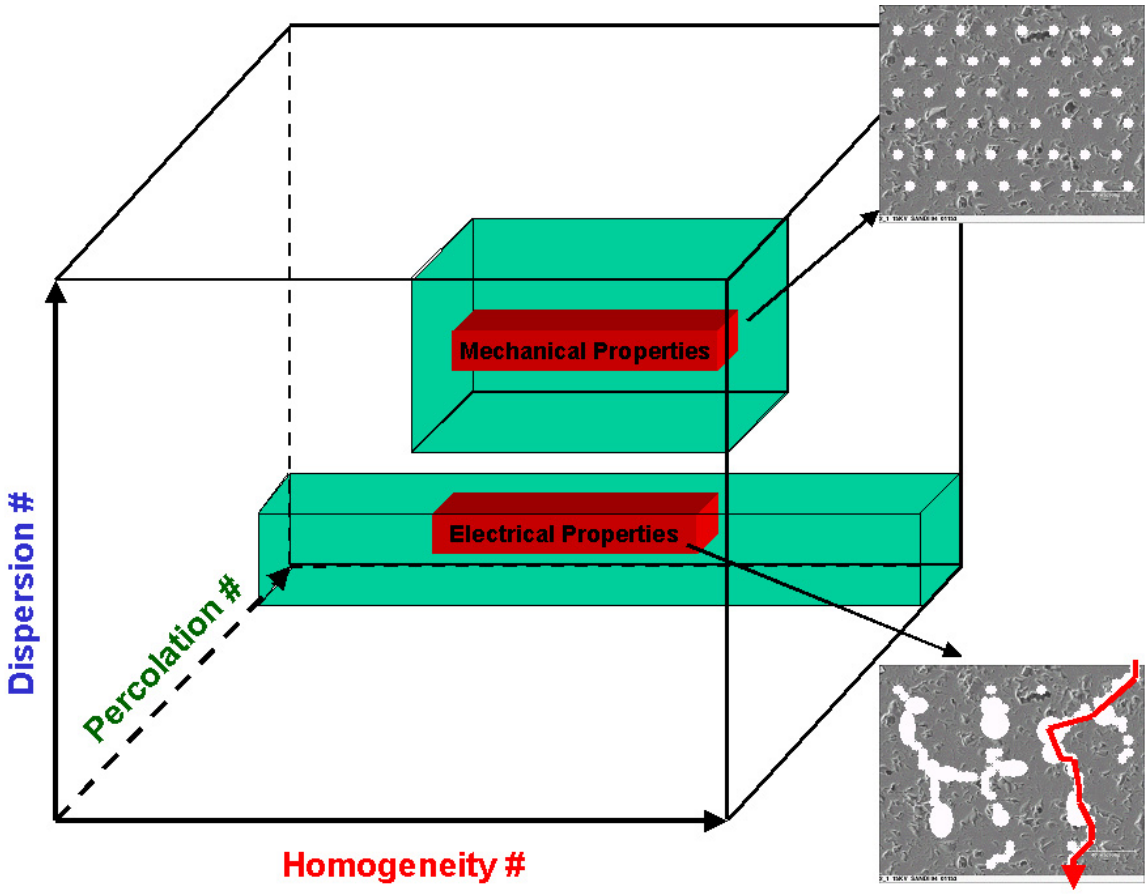

Figure 30: Physical properties of composites can be compared in three-dimensional space.

Comparison of microstructures can be accomplished several ways. Figure 31 shows four sintered, cross-sectioned, and polished cermet microstructures that have been ball milled in 250g batches at Sandia Laboratories for 0.5, 1, 4, and 20 hours. A large difference can be seen in the 20-hour ball milled sample with Mo particles agglomerating into more string-like looking areas. There is not much difference seen between the 1 or 4 hour ball-milled samples. However, when the respective indices are calculated on tessellated microstructures, the differences between the microstructures can now be seen quantitatively (Table 6). Figure 32 plots the data in Table 6 in three-dimensional space. It is believed that certain sections of this three-dimensional space would yield certain desirable properties that may not necessarily overlap.

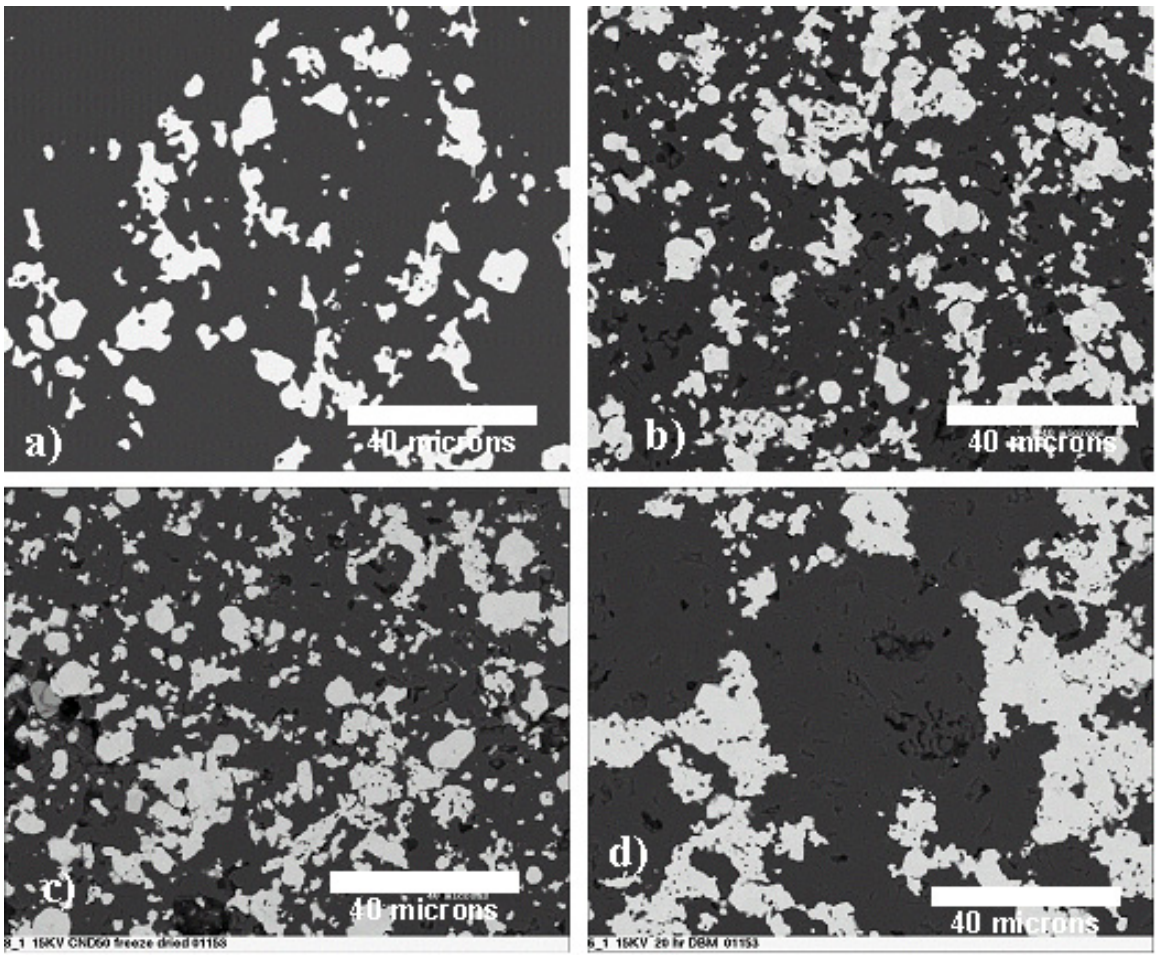

Figure 31: Microstructures of a) 0.5, b) 1, c) 4, and d) 20 hour dry-ball-milled cermet at Sandia.

Table 6: Tessellation analysis of 0.5, 1, 4, and 20 hour dry-ball-milled samples (Sandia).

DBM Time (hr)	Dispersion Index	Homogeneity Index	Percolation Index
0.5	0.939	1.495	0.1465
1	0.927	1.419	0.285
4	0.862	1.275	0.313
20	0.1	0.912	0.489

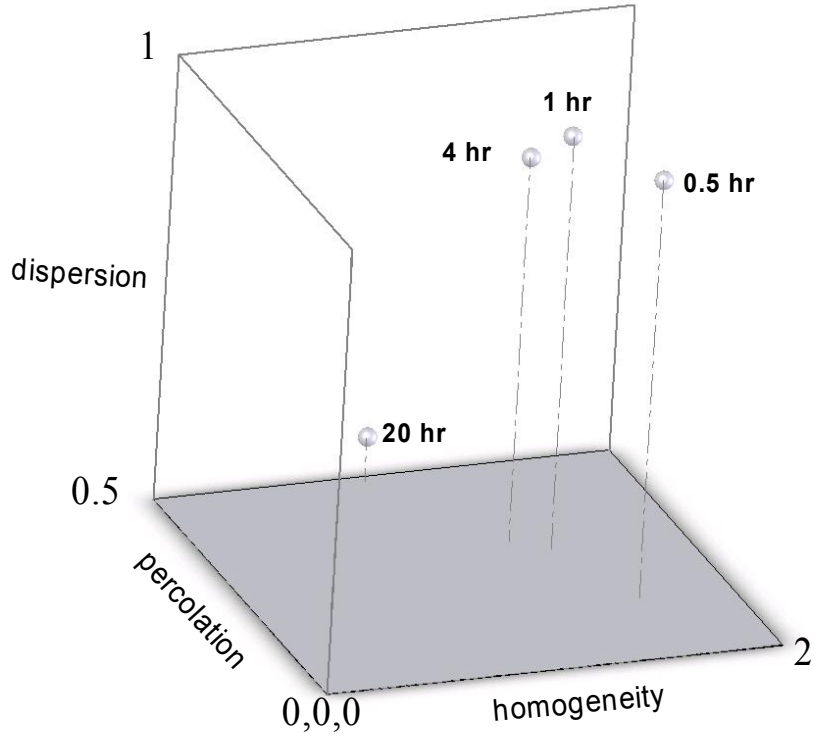

Figure 32: Dispersion, Homogeneity, and Percolation Indices 0f 0.5, 1, 4, and 20 hr DBM cermet plotted on one common graph.

9. Correlating Microstructure to Physical Properties

Microstructure characterization may be related to physical properties such as machinability and electrical resistance, both of which may be important to cermet processing. Green machine testing was performed on 30 ksi isopressed powders of 0.5, 1, 4, and 20 hour ball-mill times. The powder was pressed in 450 g batches in rubber tubes that were 0.125" thick and 1.0" inner diameter. Cermet bars were uniaxially pressed to 20 ksi in a 2" x 0.25" die and subsequently fired under standard cermet firing conditions. Six bars were made of each cermet batch with one bar used for a machinability test and five for electrical resistivity.

Machinability

Cermet cylinders were obtained from the 1.0" isopress tubes, the results of which are in Table 7. Although it is not absolutely necessary to produce a single cylinder of cermet from isopressing, a qualitative assessment of green strength can be discerned from this test. The 0.5 and 1 hour samples both yielded a single, intact cylinder, suggesting good green strength from the compaction process. The 2 and 4-hour samples cracked when being removed from the isopress tubes, suggesting a slightly lower green strength. The 20-hour sample cracked into several small pieces, which indicates poor cohesion of the compact and poor green strength.

Table 7: Isopress Results of 0.5, 1, 2, 4, and 20 hr DBM cermet.

Ball Mill Time (hr)	Result
0.5	1 piece – good
1.0	1 piece – good
2.0	2 pieces – OK
4.0	3 pieces – OK
20.0	Many pieces – poor

Green machining tests were performed on all cermet compacts.[9] A ring design was chosen as all lathe operations could be performed (turning, boring, facing, and parting). The cylinder were chucked horizontally in a lathe and faced off with diamond tooling at a feed rate of approximately 2.9 inches/minute. The diamond tool was then run on the outside of the cylinder at a feed rate of approximately 0.008" per revolution. A similar feed rate was used to diamond bore the inside. A 0.0625" diamond blade of 4" diameter mounted on an air grinder and rotating at 10,000 RPM was used to section off each part from the stock cylinder. Final green dimensions are in Figure 33.

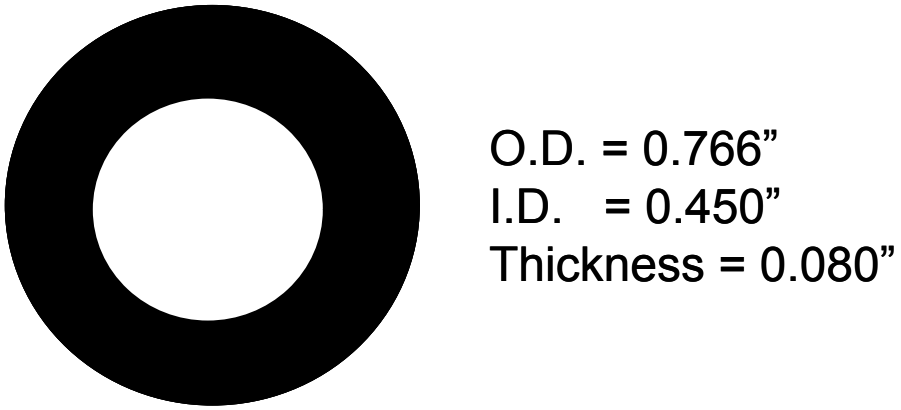

Figure 33: Schematic of a cermet ring schematic created during green machining tests.

The qualitative assessment during green machining of these cermet powder blends supports the quantitative results from microstructure characterization and qualitative results from batch isopressing. The 20 hours sample, which has the lowest dispersion and homogeneity values as well as the worst isopressing behavior (many small pieces), had the worst green machining behavior. Chipping and pullout were readily seen in the 20 hour sample, resulting in either a poor surface finish or broken parts. The 0.5 hour sample had the best green machining characteristics which is not surprising considering the low Mo content (~15 vol%) allows the sample to behave more closely to the ideal, spray-dried alumina compacts. Remaining samples, including the standard 4 hour sample, had adequate green machining characteristics, which correlates to the relatively high homogeneity and dispersion values referenced in Table 6.

Final grinding of fired cermet rings and bars produced inconclusive results. Cermet samples were ground using a diamond grinding wheel and standard grinding methods. Different thicknesses of material were removed from samples to evaluate the effects of progressive aggressive grinding on cermets. There was no difference in surface roughness of any grind when measured by a sapphire profilometer. However, laser profilometry, which is more sensitive than mechanical probes, was performed perpendicular to the grinding direction and showed the 0.5 hour sample had the highest surface roughness for the most aggressive grind (0.001”) only. An experimental variance was determined to be approximately 15%. The results of the more sensitive laser

profilometry can be found in Table 8. However, the aggressive grind produced excessive tool wear and would not be used in cermet processing, therefore, it can be concluded that cermet microstructure has no effect on final grinding results, only green machining results.

Table 8: Surface Roughness by Laser Profilometry

Ball Mill Time (hr)	Surface Roughness (μin) 0.0002" cutting depth	Surface Roughness (μin) 0.0005" cutting depth	Surface Roughness (μin) 0.001" cutting depth
0.5	0.175	0.143	0.218
1	0.118	0.196	0.140
4	0.121	0.129	0.120
20	0.124	0.155	0.147

When comparing the surface roughness values to calculated dispersion, homogeneity, and percolation indices in Figure 34, it can be seen that high percolation values and high dispersion indices correspond to poor machining (high surface roughness), which is counterintuitive to what is expected of highly dispersed and highly percolated microstructures. However, what is thought to be the more important index for machining, homogeneity, fits with theory that highly homogeneous microstructures will yield better mechanical properties (Figure 30) and therefore better machining characteristics. Standard final grinding procedures have a rough grind of 0.0005" until the final couple of machining passes, where 0.0002" is used to obtain a smooth surface finish. It can be seen in Table 8 that surface roughness is not affected by dispersion, homogeneity, or percolation, as there is no great difference between 0.5-20 hour ball milled samples. However, there may be an effect by %Mo as the 0.5-hour sample has significantly less Mo in the structure than other samples (~15% as compared to ~30% due to improper batching). Continued studies with machining and %Mo may need to be performed.

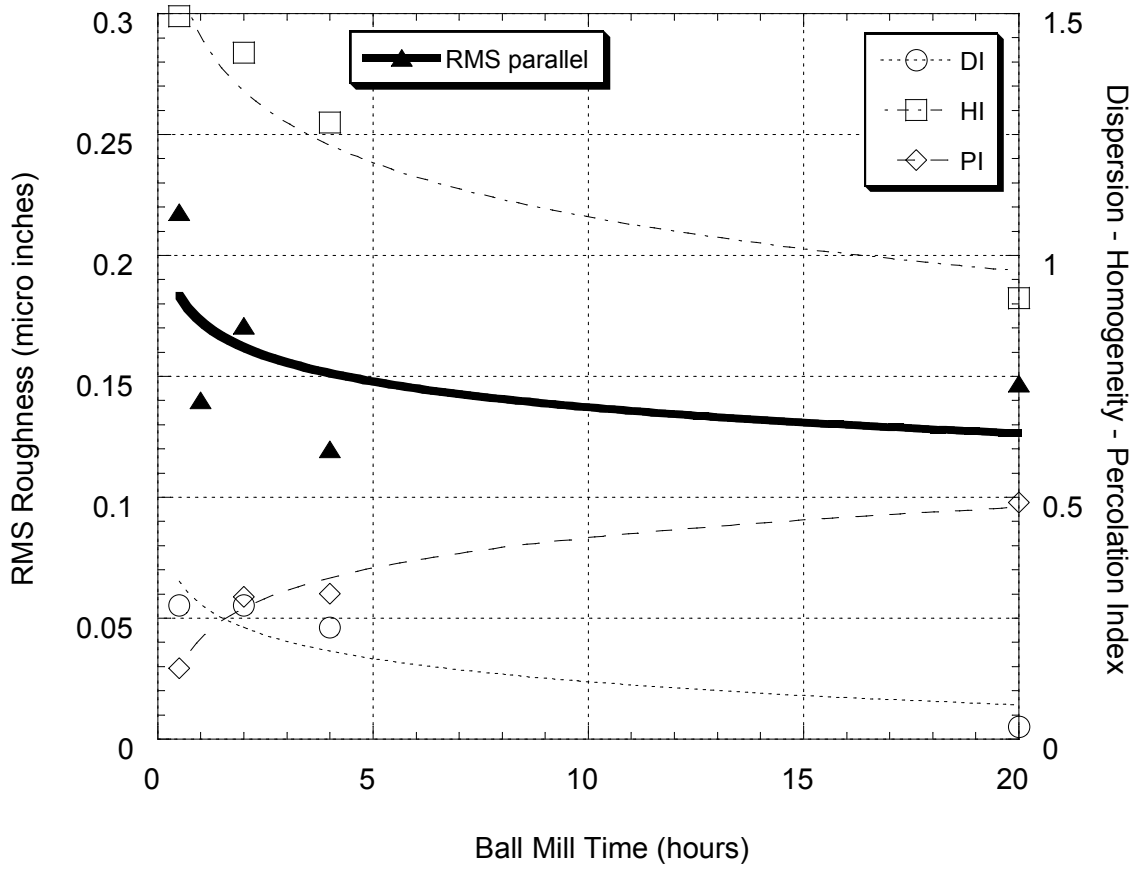

Figure 34: RMS roughness of cermet powder dry-ball milled from 0.5 to 20 hours.

Machining at CeramTec

CeramTec's Project 2A examines the machinability of samples ball milled in the larger ball-mill setup located at CeramTec, with tessellation analysis also being performed. Batches of 2.742 kg CND50 were batched and milled for 0.5, 1, 2, 4, 8, 16, and 20 hours and turned on a lathe in a manner similar to the machining test performed at Sandia. Fractionation of the standard Mo powder was performed at Fluid Energy (Hatfield, Pa), separating the small and large Mo particles. The large Mo powder batch resulted in a D90 >7.4, i.e. 90% of the particles have a particle size greater than 7.4 μm. The small powder batch had a D90 of <7.9, i.e. 90% of the particles were smaller than 7.9 μm. It is thought that CND50 with the larger Mo particles will allow for a better

percolating structure but poor machining characteristics when compared to the CND50 with the same mass of smaller Mo particles. The initial conclusions are as follows:
"1. The extended milling time offers some interesting potential benefits, although, apparently not in the area of the project. Machinability does not seem to benefit from extended milling. Machinability does not seem to benefit from increased Molybdenum size."
"2. Metallizing adherence may benefit from extended milling and from increased particle size, if the limited data we have is an indicator of Molybdenum area which in turn is an indicator of Metallizing bond strength."

Subsequent analysis of CND50 isopressed to 30 ksi yielded the following observations:
"1. With increasing milling time, we seem to have increasing Molybdenum area from 27% at 0.5 hours to 30+ % at 20 hours."
"2. With increasing milling time there is an apparent increase in standard deviation. Although these data are less believable; the trend might suggest a decrease in homogeneity with increasing milling time. The standard deviations from 2.3 at 0.5 hours to 9.1 at 15 hours and drop off to 4.2 at 20 hours."

An explanation can be offered for the change in Mo powder area percentage (total vol% has not actually changes) as a function of milling time. It has been seen that the SEM measurement of Mo area can be 'altered' to yield up to ±3% difference in the final reported value by varying the threshold values selected when separating the Mo phase from the alumina phase for a given field of view. If the contrast between the dark alumina phase and the bright Mo phase (backscattered SEM) is low, the edges between the two phases may become undistinguishable. Further, if the contrast is low, very small Mo particles may not be accounted for in the overall Mo percentage. Longer milling times tend to agglomerate the Mo particles together (Figure 29), making them more likely to be taken into account. This may explain why the longer milling times yielded a greater percentage of Mo. The greater standard deviation in data for higher ball milling times supports this explanation.

A report of the machinist's observations of the CND50 milled at various milling times is as follows:

"1. Colors of the cylinders indicate that the dispersion of the Molybdenum increases with milling time, i.e. the shade of gray gets darker as the milling time increases. This agrees with the increased Molybdenum area observed in Deliverable 2 [measurement of Mo area% with milling time]. This may also indicate that the Molybdenum is getting smaller with milling time."
"2. Machinists observations include the following: 0.5 and 1.0-hour parts seemed to lack integrity. The 2.0 and 4.0-hour parts were best: fewer chips, better surface, and more compliant. The 8.0, 16.0 and 20.0-hour samples tended to be more brittle. If there is a change in the morphology of the Molybdenum with milling time, then the binder content may be less capable."

It does not make sense to be increasing the amount of Mo by increasing milling time, making the CND50 appear a darker gray, although that is what appears to be happening. A more plausible explanation is that Mo particles are becoming more visible with time as the Sandi94 granules are broken down. Evidence of Sandi94 granule breakdown during the low energy slurry mixing can be seen in Figure 6. A darker gray color would indicate a greater mixing between alumina and Mo particles in the powder batch. From the images of these pressed and fired powders in Figure 35 and the tessellation analysis in Table 9, it can be seen that the Mo particles are most dispersed and homogeneous at times greater than 1.0 hours and less dispersed and homogeneous at the lower milling times. This would support the second observation that the 2.0 and 4.0-hour samples performed best during the green machining tests. It is unclear from these data why the longer milling times perform poorly in machining tests as the dispersion and homogeneity values are similar to shorter ball milling times. In general, the same trends were seen in the Sandia-blended CND50 where higher homogeneity and dispersion indices yielded better green-machining characteristics. It is important to note that a direct comparison cannot be made between tessellation values of the Sandia and CeramTec-processed sets of samples due to differences in magnification. It is also important to note from Table 9 that there is no significant change in molybdenum volume fraction with ball-milling time. This observation further suggests that more-intimate mixing is occurring with increased ball-milling time.

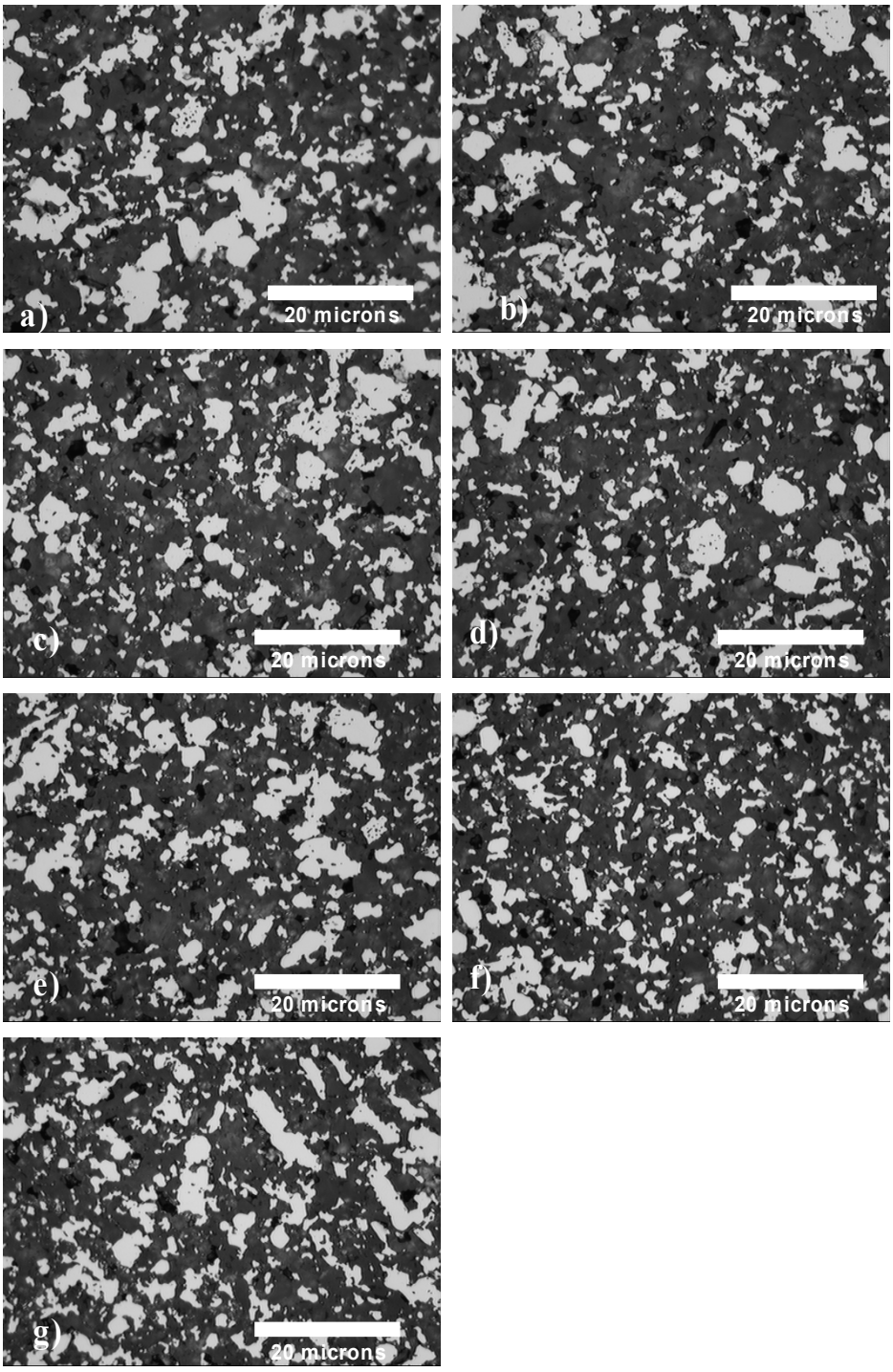

Figure 35: Microstructures of a) 0.5, b) 1.0, c) 2.0, d) 4.0, e) 8.0, f) 16.0, and g) 20.0 hour dry-ball-milled cermet at Ceramtec.

Table 9: Tessellation analysis of 0.5, 1, 2, 4, 8, 16, and 20 hour dry-ball-milled samples

DBM Time (hr)	Dispersion Index	Homogeneity Index	Percolation Index	Moly Vol. Fraction
0.5	0.293	1.425	0.322	0.2479
1	0.378	1.483	0.277	0.2216
2	0.318	12.784	0.1017	0.2699
4	0.345	12.309	0.0965	0.2549
8	0.335	12.411	0.0998	0.2645
16	0.387	13.882	0.0933	0.2474
20	0.385	12.467	0.1012	0.2652

In addition, Sandi94 was tested for green machining. Observations were as follows:

"1. Sandi94 isopresses and green machines very well. The additional binder content (3.0% Sandi94 vs. 1.5%, by weight) is likely the source of this improved performance."

"2. Machinists observations: The machining qualities of Sandi94 are desirable for Cermet machining:

A suggestion from CeramTec based on the observance of the Sandi94's performance is as follows:

"1. After milling time for cermet is reconsidered, we might consider adding organic to the dry mill to facilitate machining."

The addition of organic to facilitate green machining was validated by the non-aqueous spray drying of CND50 where it was determined that the Ethocel and Klucel E binder systems provided a cermet granule that fills dies easily, compacts well, and is easily machinable. The spray-dried cermet granules had approximately the same binder content, by volume, as the spray-dried Sandi94.

The large-sized Mo particles fractionated by Fluid Energy were evaluated for their use in cermet. The general conclusions for preliminary work suggested that larger Mo particles might be used in cermet manufacturing if the electrical properties are comparable.

Resistivity

Resistance values for 0.5, 1, 4, and 20 hour dry-ball-milled and fired cermet bars were obtained using a simple two-point probe system. Previous methods of mechanically attaching probes to cermet[11] provided inconsistent results due to the fact that additional pressure on the probes produced lower resistance values on the same sample with nominal pressure on the probes. Therefore, leads were attached to cermet with a system using conductive silver paint (SPI flash dry paint), commonly used in SEM sample preparation. Tinned copper wire (28 AWG) was held to ends of the ~ 9 x 5 x 40 mm bars and painted over with the silver paint. Once the paint had dried under atmospheric conditions, a simple digital multimeter measured resistance values to tenths of Ohms. The system resistance (two copper leads with clip ends, and 10 cm of tinned copper wire) was measured to be 0.12 Ω and is subtracted from the measured resistance values. Adjusted values are reported in Table 10. It should be noted that the resistances for the 1, 4, and 20-hour DBM samples are at the very low end of measurability for the experimental setup. Resistivity values were calculated in Table 10 from sample size and show relatively low restivities for all samples except the 0.5-hour DBM sample. The 0.5-hour DBM sample has an appreciably low percolation index, most likely due to the low Mo content due to improper batching. Therefore, the same function that gives the 0.5-hour DBM sample better green machining characteristics yields relatively poor conductivity. This is in agreement with the proposed polar properties of machinability and conductivity.

Table 10: Resistance Values of Fired Cermet

DBM time (hr)	AVG. Resistance (Ω)	Resistance Standard Deviation	AVG. Resistivity ($*10^{-5}$ Ω·cm)	Resistivity Standard Deviation
0.5	0.692	0.246	1665	591
1.0	0.052	0.010	125.3	23.6
4.0	0.034	0.005	81.3	12.03
20.0	0.056	0.005	133.0	11.56

The tessellation data from Figure 32 is plotted in Figure 36 with the resistance values as well as qualitative green machining notes beside each data point. Note again that the low percolation values correspond to high resistivity but have better machinability in the green state. Note that the 1.0 and 4.0-hour samples have both good electrical and mechanical properties as compared with the 0.5 and 20.0 hours samples, which have good mechanical and electrical properties respectively.

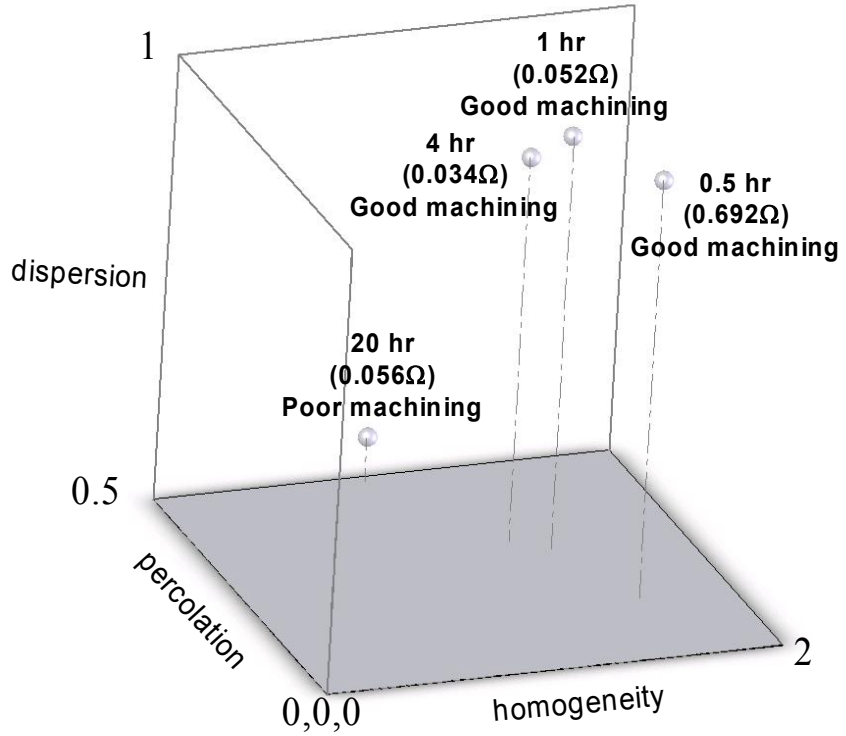

Figure 36: Correlating cermet electrical and mechanical properties to quantified microstructure. The DBM time, resistance values, and machining characteristics are given above for each data point.

Applying Machinability and Resistivity to Microstructure

From this limited study, for the best compromise of machinability and conductivity, cermet should be processed with dispersion, homogeneity, and percolation values of 0.9, 1.3, and 0.3 respectively when images are taken at a magnification of 400X. This quantification of microstructure is extremely important due to the fact that CeramTec and Sandia have different ball mill apparatus resulting in slightly different

powder morphology. The powder morphology of both systems has been matched by looking at the powder blend with an expert eye and doing subsequent tests to get a feel for the powder behavior. This method has proven useful but would be hard to repeat if system parameters in the standard-ball-mill-processing techniques were changed (such as Mo concentration), or if alternative powder-blending techniques were used (such as spray drying).

In conclusion, through the use of tessellated microstructures it is possible to relate, quantitatively, a cermet microstructure to actual physical properties regardless of processing technique. Well-dispersed and homogeneous Mo within the microstructure creates a more machinable cermet in the green state while sacrificing electrical properties. Conversely, high percolation of the Mo phase promotes good electrical properties while reducing machinability. At this initial stage of relating microstructure to physical properties, for general use, cermet should be processed to achieve microstructures with dispersion, homogeneity, and percolation values of at least 0.9, 1.3, and 0.3 respectively when images are taken at a magnification of 400X. It should be noted that these values are preliminary and may change based on further understanding of cermet performance requirements such as film deposition and brazing.

THIS PAGE INTENTIONALLY LEFT BLANK

10. Recommendations

For each work objective outlined at the beginning of this report, recommendations are summarily provided below on what has been learned, operating procedures that should be changed, and how to proceed further in investigations of each topic.

1. Increase Production Yields of Slurry-Filled Cermet Vias
   1.1. Finalized slurry filling criteria were determined, based on three designs of experiments where the following factors were analyzed: vacuum time, solids loading, pressure drop across the filter paper, slurry injection rate, via prewetting, slurry injection angle, filter paper prewetting, and slurry mixing time. Many of these factors did not have an influence on defect formation. In order of decreasing importance, critical factors for defect formation by slurry filling are vacuum time (20 sec. optimal), slurry solids loading (20.0 g of cermet with 13.00 g of DGBEA solvent (21.2 vol%)), filling with the pipette in a vertical position, and faster injection rates (~765 μl/s).
   1.2. No further recommendations for improvement to this process can be suggested.

2. Viability of High-Solids-Loading-Cermet Paste for Filling Source Feedthru Via
   2.1. The paste-filling process is easy to implement and easier to use when implemented. It is suggested that various types of solvent (including aqueous) and binder systems be investigated in conjunction with subsequent brazing and shot life testing to ensure no loss in component performance is present as compared to the slurry-filling process.
   2.2. The high stability and shelf life of the paste process lends itself to the possibility of being incorporated into a fully automated via-filling system. Here, using machine vision, parts could be randomly placed into a fixture and automatically filled.
   2.3. Other interesting points to pursue are the options of different volume fractions and sizes of molybdenum particles to enhance electrical performance.

2.4. Further, replacing molybdenum with a metal (such as iridium) that has a closer thermal expansion to that of the insulating body may allow higher levels of metal within the via, improving electrical performance.

2.5. Alternatively, a lower thermal-expansion ceramic that can be co-fired with the insulating body may be added, thereby reducing the thermal expansion of the insulating body to that of molybdenum. This would allow higher levels of molybdenum to be added to the via, again, improving electrical performance.

3. Optimize CND 50

3.1. Spray-drying and mist-granulating processes show promise in producing homogeneous, intimately mixed cermet granules that possess better flow and compaction characteristics than dry-blended CND50 powder. Improvements in binder and solvent systems should be investigated. Specifically, incorporating into the mist-granulating process the Ethocel or Klucel binder systems that showed promise in the non-aqueous-spray-drying tests.

3.2. Also, aqueous-spray drying may be a viable method to granulate powder, as there is no evidence to support the theory that oxidation present on the molybdenum particles is still present after sintering sintered in a reducing atmosphere.

3.3. Mechanical tests such as bend strength and braze buttons should be employed on all CND50 optimizing techniques to ensure no loss in mechanical performance.

3.4. Electrical tests (four point) should also be performed on all CND50 optimizing techniques.

3.5. The performance and sensitivity of the microstructure characterization technique should be evaluated specifically for electrical conductivity. Processing techniques to decrease the percolation index (lowering molybdenum content, excess ball milling, larger molybdenum particles, etc.) should be employed to determine the point where cermet is not conductive or falls below electrical conduction specifications.

References

1. J.N. Stuecker, J. Cesarano III, E.L. Corral, K.A. Shollenberger, R.A. Roach, J.R. Torczynski, E.V. Thomas, D.J. Van Ornum, *Filling Source Feedthrus With Alumina/Molybdenum Cermet: Experimental, Theoretical, and Computational Approaches*, Sandia Report SAND2006-249524951821, July 2001.
2. K.A. Shollenberger, J.R. Torczynski, J.N. Stuecker, J. Cesarano III, R. A. Roach, *Microfocus X-ray Real-Time Analysis of Slurry Flow into Cermet Vias,* Sandia Internal Memorandum to Distribution, October 10, 2001.
3. J.R. Torczynski, K.A. Shollenberger, R.A. Roach, J. Cesarano III, J.N. Stuecker, *Liquid Imbibition into Green Alumina Substrates Used to Fabricate Cermet Vias,* Sandia Internal Memorandum to Distribution, June 26, 2000.
4. K.G. Ewsuk, J. G, Arguello, *Controlling Ceramic Processing Through Science-Based Understanding and Modeling*, Sandia Report SAND 2002-2708C.
5. D. Zuech, J. Grazier, J.G. Arguello, K.G. Ewsuk, *Mechanical Properties and Shear Failure Surfaces of Two Alumina Powders In Triaxial Compression",* J. Materials Science, 36 (2001) 2911-2924.
6. K.G. Ewsuk, J. Arguello, D. Zeuch, *Characterizing and Predicting Density Gradients in Particulate Ceramic Bodies Formed by Powder Pressing,* Proceedings of the Green Body Characterization Symposium, German Ceramic Society, Koln, (2001) 169-176.
7. D.F. Susan, A.C. Kilgo, 2001, Private Communications.
8. J.R. Michael, B.B. Mckenzie, 2001, Private Communications.
9. D.J. Van Ornum, 2001, Private Communications.
10. B.B. Mckenzie, 2002, Private Communications.
11. O.M. Solomon (org 1542), *Cermet Measurements,* Sandia Internal Memorandum to R.H. Moore (org 1492), November 14, 1996.

Appendix A

Product: MC4277

WI-704191-030
Issue Date: 06/04/98
Issue B

WORK INSTRUCTION

COPY
NOT CONTROLLED

Dry Blend CND50 Powder

Change History

Section(s)	Effect.Date	Authorization	Summary
2.3, 3.1, 4.0	6/04/98	P.S. Morrison	Issue B - Under Materials, change drawing from SS443884-000 to SS305195-200 Ceramic Body, 94ND2. 3.1 Step 10 regarding labeling of ball mill cabinet door – delete step. 4.0 change drawing number on label, same as 2.3 above.

P.S. Morrison, Org 14403
Process Eng — Date

P.E. Appel, Org 14408
Quality Eng. — Date

D.L. Wallace, Org 1567
Product Eng. — Date

, Org
Title
Authorizing Signature — Date

1.0 INTRODUCTION

1.1 Scope

1.2 Purpose

To uniformly blend alumina and moly powders to form a cermet powder.

2.0 PREREQUISITES

2.1 References

Document No.	Description
DOE STD-1029-092	Writers Guide for Technical Procedures
704191-00	Feedthru
SS321504-200	Cermet Powder

2.2 Actions to be Performed Prior to Beginning Operations, where applicable

[1] Ensure traveler and paperwork agree

[2] Verify that all calibration is current

2.3 Equipment and Materials

Personal Protective Equipment		
Qty.	Equip. ID	Description
AR		Safety glasses (side shields optional)

Equipment		
Qty.	Equip. ID	Description
1		Ball milling machine
AR		Porcelain ball mill jar with lid or equivalent (dedicated to this process). Size may vary according to recipe.
AR		Al_2O_3 milling media (1/2-inch diameter by 1/2 inch long cylindrical), dedicated to this process.
AR		Polyethylene ball mill jar (dedicated to this process) Size may vary according to recipe.
AR		Spatula, non-metallic
AR		Large mesh sieve and collection pan, dedicated to this

		process. (hole size in sieve should be slightly smaller than milling media size)
1		Balance
1		Timer (optional)
1		Flow Hood
1		Artist brush, dedicated to this process (optional)
AR		Glass, nalgene, or polypropylene jar with lid for storage

Materials		
	Dwg./Part Number	Description
AR	SS305195-200	Ceramic Body, 94ND2
AR	SS704715-000	Molybdenum powder

Shop Supplies		
	Dwg./Part Number	Description
AR		Gloves or finger cots
AR		Patapar paper or weighing boats
AR		Shop towels
AR		Container label

2.4 Records

Traveler, Source Feedthru

2.5 Waste Management

Any waste generated as a result of this process will be handled according to the appropriate ES&H Manual chapter.

3.0 PROCEDURE

Note:

For purposes of clarification, when the term "ball mill" jar is used, it refers to either a porcelain or a polyethylene jar. Either jar is acceptable for this process.

3.1 Preparation

[3] Fill ball mill jar approximately 1/3 full with alumina milling media.

Note:

For the alumina powder, secondary powder (fines) are preferred, but not required.

[4] Place clean patapar paper or weighing boat on balance and tare it's weight.

Note:

Recipe may be incrementally multiplied in 500.0-gram units (total powder) per liter or quart mill jar size.
Example: 1000.0g total powder in a 2-liter milling jar

[5] Weigh out 250.0-grams ± 0.2-grams of alumina powder.

[6] Pour into 1-liter ball mill jar.

[7] Place clean patapar paper or weighing boat on scale and tare it's weight.

[8] Weigh out 250.0-grams ± 0.2-grams of Moly powder.

[9] Pour into the ball-milling jar.

Caution:
Do not load or unload ball-milling machine while it is turned on.

[10] Place jar in ball milling machine. Verify the jar is resting level and not slipping on the rollers

[11] Mill for minimum of 2 hours. Use of a timer is optional.

[12] After 2 hours, remove jar from milling machine and check the powder.

CND50 should be uniformly gray with no visible segregation of alumina. If separate white and gray areas are observed then replace jar in milling machine and continue milling until a uniform color is achieved.

[13] In a flow hood environment, pour powder and milling media onto sieve and collect the powder in pan underneath. The large mesh sieve is for capturing the milling media.

Optional: An artist brush may be used to assist in collecting the powder in the pan, do not allow loose bristles to contaminate powder.

[14] Affix label to storage jar. Indicate the tare weight of the jar, date, alumina powder lot number, Moly lot number, and amounts of alumina and Moly in CND50. Place lid on jar and store in controlled cabinet 878/Y715.

[15] Sign traveler.

[16] Notify document control in building 878 when dry blending of the CND50 powder is complete.

[17] Milling media should be cleaned with water before the next batch.

4.0 APPENDIX

CERMET POWDER

SS321504-200 _____
SS305195-200 _____
Ceramic Body, 94ND2
Alumina Powder Lot _____
Amt. _____g

SS704715-000 _____
Molybdenum Powder
Lot _____
Amt. _____g

CND50 Batch Lot # _____

Date ____/____/____ Initials _____

Jar tare wt., w/o lid = _____g

APPENDIX A
CHANGE HISTORY

Section(s)	Effect.Date	Authorization	Description
All	4/30/98	P.S. Morrison	Issue A – Initial release
2.3, 3.1, 4.0	6/04/98	P.S. Morrison	Issue B - Under Materials, change drawing from SS443884-000 to SS305195-200 Ceramic Body, 94ND2. 3.1 Step 10 regarding labeling of ball mill cabinet door – delete step. 4.0 change drawing number on label, same as 2.3 above.

Appendix B

Product: MC4277

WORK INSTRUCTION

COPY
NOT CONTROLLED

CND50 Slurry Preparation

Change History

Section(s)	Effect.Date	Authorization	Summary
All	4/30/98	P.S. Morrison	Issue A – Initial release
2.3, 2.4, 3.1	5/18/98	P.S. Morrison	Issue B – 2.3 Add side shields optional w/safety glasses. Add 1 ea calibrated timer. 2.4 Delete NCR records. 3.1 After Step 9, add note to calibrate mixer before use with timer and count revolutions. Step 13 Add to notify document control when process is completed.

P.S. Morrison, Org 14302
Process Eng
Date

P.E. Appel, Org 14408
Quality Eng.
Date

D.L. Wallace, Org 1567
Product Eng.
Date

, Org
Title
Authorizing Signature
Date

1.0 INTRODUCTION

1.1 Scope

1.2 Purpose

To uniformly mix CND50 slurry

2.0 PREREQUISITES

2.1 References

Document No.	Description
DOE STD-1029-092	Writers Guide for Technical Procedures
704191-00	Feedthru
SS443970-200	Cermet Slurry

2.2 Where applicable, actions to be Performed Prior to Beginning Operations

[1] Ensure travelers accompany parts and assemblies and that parts and paperwork agree

[2] Verify that the previous sequence (if applicable) has been completed and verify quantity

[3] Verify that all calibration is current and calibrate at time of use is accomplished.

2.3 Equipment and Materials

Personal Protective Equipment		
Qty.	Equip. ID	Description
AR		Safety glasses (side shields optional)

Equipment		
Qty.	Equip. ID	Description
AR		Slurry pot with lid
AR		Tilted mixer (Calibrate at time of use)

1		Balance
AR		Stainless steel balls (1/2 inch)
AR		Stainless steel balls (3/8 inch)
AR		Stainless steel balls (1/4 inch)
AR		Weighing boat
AR		Finpippette, eyedropper, or syringe with disposable tip
1		Graduated cylinder, capable of volume to 15ml
AR		Spatula, non-metallic
1		Timer, calibrated

Materials		
	Dwg./Part Number	Description
AR	SS305003-200	DGME acetate
AR	SS321504-201	CND50 powder
AR		(Nuosperse 657) Surfactant
AR		Methanol, reagent grade or better

Shop Supplies		
	Dwg./Part Number	Description
AR		Paper towels
AR		Gloves/finger cots (optional)
AR		Patapar paper

2.4 Records

Traveler, Source Feedthru (TR-704191)

Data Form (DF-CER-001)

2.5 Waste Management

Paper towels contaminated with CND50 slurry and methanol will be handled according to the appropriate ES&H Manual chapter.

3.0 PROCEDURE

3.1 Preparation

[4] Before beginning process, fill in the required information on the Data Form. The Data Form should accompany the Traveler.

[5] Place weighing boat or patapar paper on balance and tare.
Weigh out 20 ± 0.2 grams of CND50 powder.

[6] Place powder into slurry pot containing Stainless steel balls (3 each: ½ inch, 3/8 inch, and ¼ inch Stainless steel balls).

[7] Add 7-12 ml DGME to slurry pot using either a graduated cylinder, Finpippette, or syringe.

[8] Place 2 or 3 drops of Nuosperse into pot using eyedropper.

[9] Cover pot and place pot onto shaft of mixer.

Note:

To calibrate mixer at time of use: Use timer and count revolutions.

[10] Blend mixture for a minimum of ½ hour at 60 rpm ± 10 rpm, to create smooth uniform slurry.

[11] After using slurry, clean mixing pots and stainless steel balls with methanol and paper towels.

[12] Sign Traveler.

[13] Notify document control in building 878 when process is completed.

4.0 APPENDIX

APPENDIX A
CHANGE HISTORY

Section(s)	Effect.Date	Authorization	Description
All	4/30/98	P.S. Morrison	Issue A – Initial release
2.3, 2.4, 3.1	5/18/98	P.S. Morrison	Issue B – 2.3 Add side shields optional w/safety glasses. Add 1 ea calibrated timer. 2.4 Delete NCR records. 3.1 After Step 9, add note to calibrate mixer before use with timer and count revolutions. Step 13 Add to notify document control when process is completed.

Distribution:

1	MS 1349	01815	J. N. Stuecker
1	MS 1349	01815	J. Cesarano III
1	MS 1349	01815	W. H. Hammetter
1	MS 0886	01822	A. C. Kilgo
1	MS 0886	01813	D. F. Susan
1	MS 0959	02454	S. T. Reed
1	MS 0834	02732	R. A. Roach
1	MS 0612	09612	Review and Approval Desk, For DOE/OSTI
2	MS 0899	09616	Technical Library
1	MS 9018	89451	Central Technical Files
1	MS 0869	027221	T. M. Stephens
1	MS 0561	027221	D. J. Van Ornum